Emission of Particles Following Muon Capture in Intermediate and Heavy Nuclei*

PAUL SINGER

Contents

I. Introduction

The purpose of this talk is to present a review of theoretical work and experimental results of recent years on the emission of particles from nuclei, following muon capture. As emphasized in the title, my lecture is restricted to intermediate and heavy nuclei, so as to minimize the overlap with Professor Überall's report [81]. Even so, for the sake of continuity, I am afraid that both of us will have to "intrude" occasionally into the other's domain.

The topic of my review is, I believe, customarily classified today as belonging to "intermediate energy nuclear physics" and has been succinctly covered in conferences dealing with "High Energy Physics and Nuclear Structure". Indeed, the study of the particles emitted after muon capture provides an additional angle for obtaining information on nuclear structure. The usefulness of the muon in this respect is enhanced when considered together with the analysis of other "particle physics tools", like K^- and π^- meson capture, pion photoproduction from nuclei, etc.

* Review talk presented at the Muon Physics Conference, Colorado State University, Fort Collins, Colorado, 6–10 September, 1971 (Expanded and updated version, September, 1973).

II. Neutron Emission

2.1 General

The basic process we consider is the capture of a muon by a nucleus from a K-atomic orbit. As a result of the weak interaction the following nuclear reaction occurs:

$$\mu^- + A_Z^N \rightarrow \nu_\mu + X\,. \tag{1}$$

The detectable product X consists of a residual heavy nucleus and light particles. In intermediate and heavy nuclei, the light particles are neutrons and (or) γ's in most of the cases. The few percent of charged light particles observed are mainly protons, but deuterons and α-particles have also been observed in still smaller quantities. In the following, we address ourselves to the question of neutron emission.

The average number of neutrons emitted per capture increases with the atomic number. The experimental figures [1] for a sample of naturally occurring elements ranging from Al to Pb are as follows:

Table 1

	Al	Si	Ca	Fe
Average number of neutrons per capture	1.26 ± 0.06	0.86 ± 0.07	0.75 ± 0.03	1.12 ± 0.04
	Ag	I	Au	Pb
	1.61 ± 0.06	1.44 ± 0.06	1.66 ± 0.04	1.71 ± 0.07

The increase in the average multiplicity of neutrons is however only a rough description, and the deviations from a smooth line, due to particular nuclear structure effects, are quite large.

Bobodyanov has pointed out [83] that the general trend of ν (= average number of neutrons per capture) is described well by the empirical function $\nu = (0.3 \pm 0.02)\, A^{1/3}$.

The emission of neutrons can be approximately classified as direct or from an intermediate "compound nucleus" formed after the muon capture process. Direct emission refers to the neutron created in the elementary process

$$\mu^- + p \rightarrow n + \nu_\mu\,, \tag{2}$$

which succeeds in leaking out of the nucleus. These neutrons have fairly high energies, from a few MeV to as high as 40–50 MeV [2–5].

The direct neutrons are expected to carry with them information on the basic process (2), like angular asymmetry with respect to the muon spin as a result of parity violation in the weak interaction.

Most of the neutrons emitted after capture seem however to be "evaporation neutrons". In intermediate and heavy nuclei the excitation energy acquired by the neutron formed in the capture process is shared with the other nucleons of the nucleus and a "compound nucleus" is formed. This intermediate excited nuclear state then loses energy by boiling-off mainly low-energy neutrons.

Some authors (e.g. Ref. [3]) distinguish between direct neutrons, evaporation neutrons and giant-resonance neutrons. The latter are the neutrons emitted following a capture process in which transitions to giant multipole nuclear levels play an important role [6, 7]. This manifestation of the nuclear giant resonance levels and the relation of muon capture to photoproduction by using the conserved vector current theory has been considered mainly with reference to light and intermediate nuclei [8]. The possibility of detecting typical "giant-resonance" neutrons in particular in intermediate and heavy nuclei, is however not a necessary corollary of the fact that the capture mechanism proceeds through these collective states. The de-excitation of the giant-multipole states, which occur in intermediate nuclei at excitation energies of 15–25 MeV, will most probably occur through a statistical boiling-off process. In Ca^{40} for instance, where the giant-dipole states are responsible for approximately 55% of the capture rate [7], some 80–90% of the neutrons emitted follow an evaporation spectrum, on top of which there is also evidence [5, 9] of a line spectrum indicative of transitions between resonant ^{40}K to excited ^{39}K. In lighter nuclei, it would be more feasible to detect line transitions from the giant resonance states.

2.2 Neutron Evaporation and Neutron Multiplicities

If the process (2) occurs with a proton at rest, the resulting neutron carries an energy of $E_n \simeq \mu^2 c^2/2M_n \simeq 6\,\text{MeV}$. The nuclear protons have however a finite momentum distribution, and the neutrons can therefore emerge from the capture reaction with a spectrum of energies. In order to account for the low energy neutrons emitted after muon capture, the following physical picture [10] involving a two-step process can be used: the muon is captured by a quasi-free nucleon, whose acquired energy is distributed among the nucleons of the nucleus, and a compound nucleus is thus formed:

$$\mu^- + A_Z^N \rightarrow \nu_\mu + (A_{Z-1}^{N+1})^* \tag{3}$$

The excited nuclear state then loses energy by evaporating nuclear particles (mainly neutrons) and γ-rays till a ground state is reached.

$$(A_{Z-1}^{N+1})^* \rightarrow A_{Z-1}^{N+1} + \gamma\text{'s} \tag{4a}$$

$$\rightarrow A_{Z-1}^{N} + n + \gamma\text{'s} \tag{4b}$$

$$\rightarrow A_{Z-1}^{N-1} + 2n + \gamma\text{'s} \quad \text{etc.} \tag{4c}$$

This picture is expected to be of greater validity for heavier nuclei.

McDonald, Kaplan, Diaz, and Pyle [1, 11] have done the first extensive experiments to measure the neutron multiplicity distributions from μ^- capture in several intermediate and heavy nuclei. In their experiment, the neutrons emitted after μ^- capture are first thermalized and then detected by using a cadmium-loaded liquid-scintillator tank. In Fig. 1 we give the results of McDonald, Kaplan, Diaz, and Pyle for the emission of 0, 1, 2, ... neutrons after muon capture in various nuclei. The F_i are the multiplicities corrected for the experimental detection efficiency of the neutron counter (54.5%).

If the degenerate Fermi gas picture is used for the nucleons, the resultant excitation gives an average emission of neutrons of about half the observed one [11]. Moreover, no evaporation of 3 or 4 neutrons, as observed to occur in a certain percentage, is then accountable. A more realistic description of the capturing nucleus is obviously needed in order to calculate the nuclear excitation. As the process under consideration is mainly a volume effect, the Brueckner picture [12] for the constant-density region of the heavy nuclei can be used [13]. The nucleons are described as moving most of the time independently in a momentum-dependent average potential $V(p)$ created by the other nucleons. The momentum dependence of $V(p)$ is nearly quadratic for momenta lower than the Fermi momentum. The capturing nucleon can then be treated by using an effective mass

$$M^*(p) = p/(dE/dp) .$$

From the $E(p)$ calculated for nuclear matter [12], one deduces for $p < p_F$

$$M^* = M\,(0.60 + 0.13\,p^2/p_F^2) ,$$

while for $p > p_F$, $M^*(p) \rightarrow M$. For finite nuclei, the effective mass might be even smaller [14]. The use of the effective mass approximation thus accounts for an increased excitation energy from the capture process.

A second improvement to be made is the use of a more realistic momentum distribution for the nucleons in the nucleus. Evidence from a wide range of phenomena reveals [13] that the nucleon

Target	Average multiplicity,	Multiplicity distribution (adjusted to 0.545 efficiency)							
		F_0	F_1	F_2	F_3	F_4	F_5	F_6	F_7
Al	1.262 ± 0.059	0.449 ± 0.027	0.464 ± 0.028	0.052 ± 0.013	0.036 ± 0.007	-0.0023 ± 0.004	-0.001 ± 0.004	0.003 ± 0.004	
Si	0.864 ± 0.072	0.611 ± 0.042	0.338 ± 0.042	0.045 ± 0.018	-0.002 ± 0.008	0.003 ± 0.005	0.002 ± 0.005	0.003 ± 0.006	
Ca	0.746 ± 0.032	0.633 ± 0.021	0.335 ± 0.022	0.025 ± 0.009	0.004 ± 0.006	0.003 ± 0.003			
Fe	1.125 ± 0.041	0.495 ± 0.018	0.416 ± 0.019	0.074 ± 0.011	0.014 ± 0.005	-0.0001 ± 0.003	0.002 ± 0.003		
Ag	1.615 ± 0.060	0.360 ± 0.021	0.456 ± 0.023	0.144 ± 0.017	0.031 ± 0.009	0.007 ± 0.005	0.002 ± 0.004	0.001 ± 0.003	
I	1.436 ± 0.056	0.396 ± 0.021	0.474 ± 0.023	0.087 ± 0.015	0.035 ± 0.009	0.007 ± 0.005	0.0002 ± 0.004		
Au	1.662 ± 0.044	0.370 ± 0.015	0.425 ± 0.016	0.156 ± 0.012	0.032 ± 0.006	0.014 ± 0.004	0.003 ± 0.003	0.0003 ± 0.003	
Pb	1.709 ± 0.066	0.324 ± 0.022	0.483 ± 0.025	0.137 ± 0.018	0.045 ± 0.010	0.011 ± 0.006			
Ag	1.60 ± 0.18	0.389 ± 0.100	0.455 ± 0.075	0.120 ± 0.035	0.030 ± 0.015	0.001 ± 0.003	0.009 ± 0.006	0.000 ± 0.007	0.010 ± 0.007
Pb	1.64 ± 0.16	0.348 ± 0.100	0.479 ± 0.057	0.137 ± 0.027	0.018 ± 0.012	0.010 ± 0.005	0.005 ± 0.004	0.003 ± 0.002	0.002 ± 0.002

Fig. 1. The multiplicity distribution and the average neutron emission from the experiment of MacDonald et al. [1]. The last two items of the table refer to their previous experiment [11].

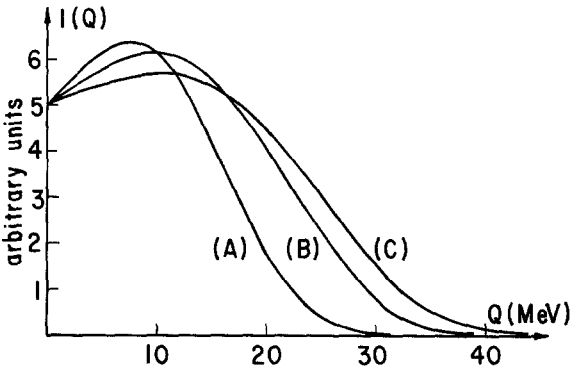

Fig. 2. The nuclear excitation distribution in Ag^{107}, calculated [13] for three choices of the effective mass and the Gaussian momentum distribution parameter: (A) $M^* = M$; $\alpha^2/2M = 14$ MeV. (B) $M^* = 0.68\,M$; $\alpha^2/2M = 14$ MeV. (C) $M^* = 0.68\,M$; $\alpha^2/2M = 20$ MeV

momentum distribution $\varrho(p)$ is well approximated by

$$\varrho(p) = N \exp\left[-p^2/\alpha^2\right], \tag{5}$$

with

$$15\ \text{MeV} < \alpha^2/2M < 20\ \text{MeV}.$$

The above two effects were taken [13] into account in calculating the nuclear excitation distribution $I(Q)$, and the result for Ag^{107} is shown in Fig. 2. In the calculation, the excitation energy

$$Q = {}_A(Mc^2)^Z - {}_A(Mc^2)^{Z-1} + \mu c^2 - B_\mu - k_\nu c \tag{6}$$

is related to the capturing process by

$$Q = (2M^*)^{-1}(q^2 - p^2), \tag{7}$$

where q, p are the momenta of the neutron and proton involved in (1). The Pauli principle effect is taken into account in the calculation of $I(Q)$. In Fig. 3 the difference between the excitation functions in Au^{197} obtained [1] with various momentum distributions for the nucleons is exhibited (the effective masses used were chosen so as to give the observed *average* neutron emission).

The emission of neutrons from the excited nucleus is calculated [1, 11, 13] by using the statistical theory of Weisskopf and Ewing [15]. The missing accurate knowledge of the level density of the nuclei involved has been replaced in the above calculations by the assumption of an evaporation spectrum for the emitted neutrons

$$dN(E) \sim E \exp\left[-E/\theta\right] dE. \tag{8}$$

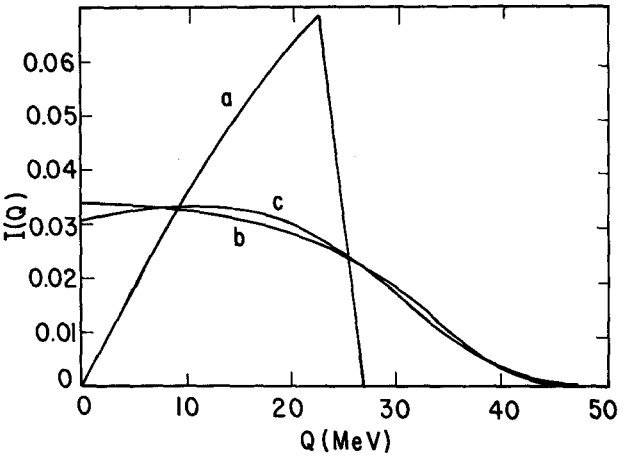

Fig. 3. The nuclear excitation distribution in Au, calculated [1] for various effective masses and momentum distributions: a $M^* = 0.38\,M$; Fermi gas, $\theta_f = 0$. b $M^* = 0.25\,M$; Fermi gas, $\theta_f = 12$ MeV. c $M^* = 0.46\,M$; Gaussian, $\alpha^2/2M = 20$ MeV

Using information from nuclear reactions at comparable energies, constant nuclear temperatures were used in the calculations [1, 13] with $\theta = 0.65 - 0.75$ MeV. Small changes in θ do not significantly affect the calculations.

Using a Gaussian momentum distribution with $\alpha^2/2M = 20$ MeV and an average effective mass of $M^* = 0.68\,M$, one finds that the theoretical prediction [13] is only in rough agreement with experiment (Fig. 4). The calculated average emission is generally 20% lower than observed and the agreement with experiment for f_0 and f_1, is generally poor.

One can improve the agreement by considering smaller effective nucleon masses. If the effective mass for Ag, I, Au, Pb is chosen to be $M^* \simeq 0.5M$, then the observed average neutron emission is well reproduced [1], but the multiplicity distributions calculated are still not in good agreement with experiment, especially for f_0 and f_1 (Fig. 5).

In the work of Kaplan et al. [1, 11] there is no experimental distinction between direct and evaporated neutrons. Hence, in comparing with their experiment, one should include in the calculation the appropriate percentage of neutrons directly emitted. When this is done, by assuming approximately 15–20% probability for neutrons to be emitted directly [13], the agreement of the calculation with experiment is generally improved. In order to reproduce the observed average neutron emission an effective mass $M^* \simeq 0.4M$ is now required in

Neutron multiplicities	Ag		I	
	Calculated	Experimental	Calculated	Experimental
f_0	0.488	0.383 ± 0.025	0.492	0.393 ± 0.026
f_1	0.372	0.455 ± 0.025	0.369	0.463 ± 0.026
f_2	0.119	0.124 ± 0.015	0.118	0.107 ± 0.014
f_3	0.020	0.033 ± 0.007	0.020	0.029 ± 0.007
f_4	0.001	0.002 ± 0.003	0.001	$0.007 \pm 0.004'$
f_5	—	0.002 ± 0.002	—	0.000 ± 0.002
f_6	—	0.001 ± 0.001	—	—
n	0.674	0.827 ± 0.032	0.669	0.792 ± 0.032
ν	1.27	1.55 ± 0.06	1.26	1.49 ± 0.06
	Au		Pb	
f_0	0.466	0.368 ± 0.022	0.454	0.376 ± 0.027
f_1	0.373	0.447 ± 0.023	0.378	0.446 ± 0.028
f_2	0.135	0.144 ± 0.014	0.143	0.121 ± 0.016
f_3	0.024	0.027 ± 0.006	0.024	0.049 ± 0.010
f_4	0.002	0.011 ± 0.003	0.001	0.007 ± 0.004
f_5	—	0.002 ± 0.002	—	0.002 ± 0.002
f_6	—	—	—	—
n	0.722	0.870 ± 0.029	0.740	0.873 ± 0.037
ν	1.36	1.63 ± 0.06	1.40	1.64 ± 0.07

Fig. 4. Comparison of the calculated [13] neutron multiplicities with the experiments of Kaplan et al. [1, 11] (assuming a Gaussian momentum distribution with $\alpha^2/2M = 20$ MeV and $M^* = 0.68\,M$)

heavy nuclei. A further improvement is obtained when the emission of neutrons from the nuclear surface due to the pseudodeuteron effect [16] is also included in the calculation. As can be seen by comparing Fig. 1 and Fig. 6, the agreement for Ag is now fair, for a Gaussian distribution with $\alpha^2/2M = 20$ MeV, $M^* = 0.39\,M$, direct volume emission of 22% and clustering parameter of 0.14.

Further to the early radiochemical methods [17] for identifying the radioactive products following muon capture and the direct measurements of the emitted neutrons of Kaplan et al. [11, 1] with a high-efficiency detector, a third generation of detailed experiments [18–22, 84–87] has recently been started in which the γ-rays following μ-capture are detected. Since in most cases one would expect the nucleus to be left in an excited state after emitting a neutron, or even when capture occurs without neutron emission, the multiplicity distribution of neutron-emission can be obtained from the identification of the isotopes detected through their γ-emission. These nuclear γ-rays are delayed with respect to the X-rays because of the finite lifetime of the muon in the atomic $1S$ level. The main disadvantage of

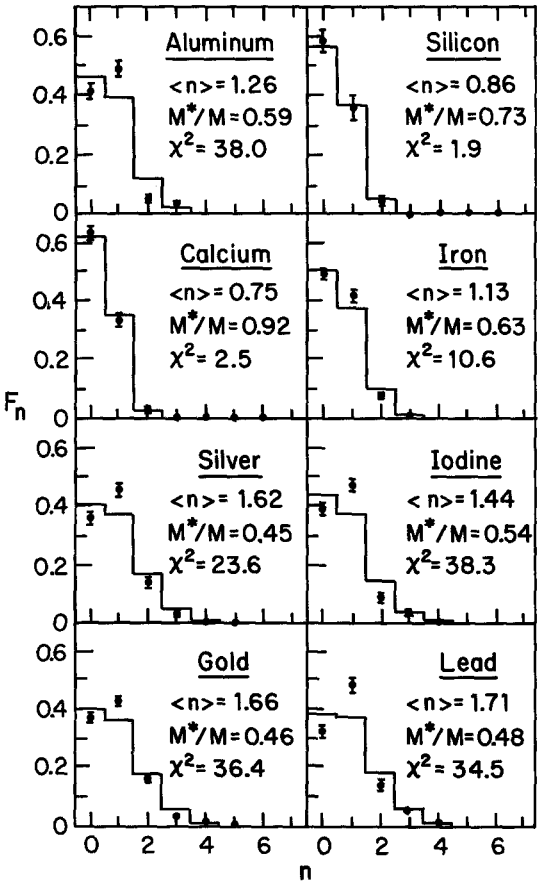

Fig. 5. Comparison of the calculated [1] neutron multiplicities with experiment [1], by using a Gaussian momentum distribution with $\alpha^2/2M = 20$ MeV and effective masses chosen as to give the experimental average multiplicity

this method is that one cannot detect neutron emission leading to the ground state of the residual nucleus. On the other hand, one can measure directly the non-neutron capture events by detecting the γ-rays from the excited$_{Z-1}A^{N+1}$ nucleus appearing after μ-capture. Moreover, this method allows of a direct measurement of the relative occurrence of various excited states appearing in the process.

Backenstoss et al. [18] have measured the nuclear γ-rays after muon capture in several odd-A, odd-Z isotopes $-{}^{45}_{21}$Sc, ${}^{55}_{25}$Mn, ${}^{59}_{27}$Co, ${}^{93}_{41}$Nb, ${}^{127}_{53}$I, and ${}^{209}_{83}$Bi, Petitjean et al. [19] in ${}^{151}_{63}$Eu and ${}^{153}_{63}$Eu and Kessler et al. [20] in ${}^{89}_{39}$Y. The comparison for the neutron multiplicities obtained in the first two experiments with calculations based on the

Target	Direct-emission parameter	Clustering parameter	Effective mass M^*/M	Multiplicity distribution x^2	P_0	P_1	P_2	P_3	P_4	P_5
Fermi gas, $\theta_f = 0$ MeV										
Ag	0.216	0	0.43	4.7	0.343	0.463	0.166	0.029		
I	0.199	0	0.45	20.2	0.378	0.474	0.136	0.012		
Au	0.157	0	0.34	27.9	0.333	0.458	0.179	0.030		
Pb	0.153	0	0.32	15.2	0.320	0.459	0.190	0.030		
Ag	0.216	0.144	0.45	9.5	0.333	0.472	0.175	0.019		
Fermi gas, $\theta_f = 12$ MeV										
Ag	0.216	0	0.26	24.4	0.409	0.377	0.151	0.054	0.009	0.001
I	0.199	0	0.30	32.2	0.442	0.380	0.135	0.039	0.004	
Au	0.157	0	0.19	41.5	0.407	0.364	0.158	0.058	0.011	0.001
Pb	0.153	0	0.18	35.7	0.394	0.368	0.165	0.060	0.012	0.001
Ag	0.216	0.144	0.29	11.8	0.388	0.397	0.167	0.041	0.006	
Gaussian, $\alpha^2/2M = 20$ MeV										
Ag	0.216	0	0.36	22.3	0.407	0.380	0.149	0.053	0.009	0.001
I	0.199	0	0.46	29.6	0.441	0.384	0.133	0.038	0.004	
Au	0.157	0	0.40	32.7	0.401	0.373	0.160	0.056	0.010	0.001
Pb	0.153	0	0.41	30.4	0.387	0.377	0.167	0.057	0.011	0.001
Ag	0.216	0.144	0.39	10.5	0.387	0.400	0.166	0.041	0.006	

Fig. 6. Multiplicity distributions calculated [1] with the inclusion of direct volume and surface emission [13]

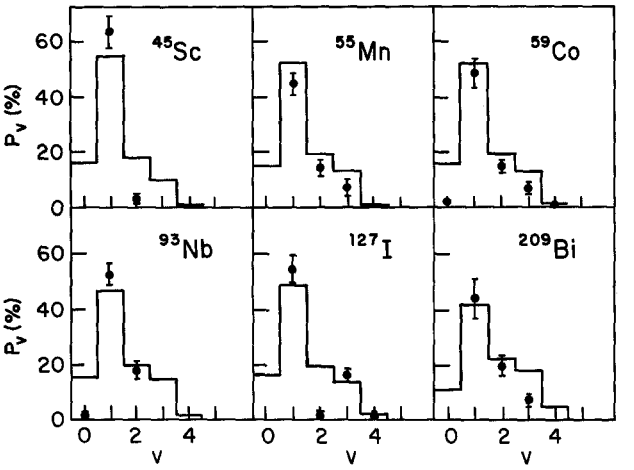

Fig. 7. The experimental values of the neutron multiplicities for several nuclei, found by γ-ray detection [18], compared with the predictions based on the model of Ref. [13]. Parameters used in the calculation: Gaussian momentum distribution with $\alpha^2/2M = 20$ MeV, $M^* = 0.5\,M$, nuclear temperature $\theta = 0.75$ MeV

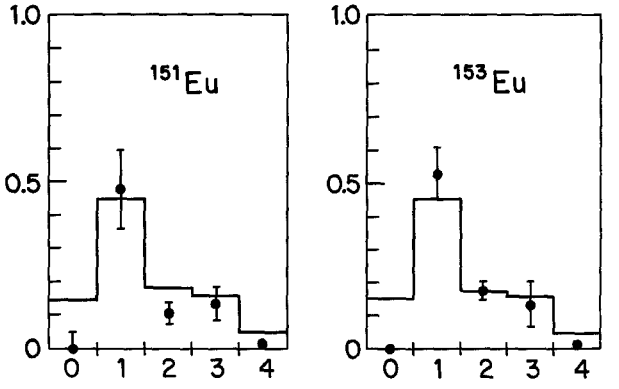

Fig. 8. The experimental values of the neutron multiplicities for $^{151}_{63}$Eu and $^{153}_{63}$Eu found by γ-ray detection [19], compared with the predictions based on the model of Ref. [13]. Parameters used in the calculation: Gaussian momentum distribution with $\alpha^2/2M = 20$ MeV, $M^* = 0.5\,M$, nuclear temperature $\theta = 0.75$ MeV

model of Ref. [13] is given in Figs. 7 and 8. In the calculation the direct nucleon emission has been included (though not any surface effects [16]), along with the evaporation neutrons. These experiments indicate practically zero probability for no-neutron emission for all the nuclei studied, while the theoretical calculation predicts 15–18% for it. On the other side, the agreement with the calculated multiplicity distributions for emission of one or more neutrons is quite good.

Additional experiments which detect the delayed γ-ray emission following μ-capture have been performed recently by Evans [84], Temple et al. [85] and Miller et al. [86, 87]. Evans [84] has studied a large number of nuclei, including Si, Ti, Mn, Fe, Co, Ni, Y, Ag and Au, however his findings are not sufficient for drawing any conclusions on the neutron distribution. Temple et al. [85, 86] have analyzed the delayed γ-nuclear emission following μ-capture in Al, Si, Ca, and Co and have concentrated on studying the nuclear structure by comparison with other excitation reactions in appropriate nuclei. The lower limits they were able to establish on neutron multiplicities are consistent with the data of Ref. [1]. Miller et al. have used the delayed γ-ray technique to study both light-intermediate [86] ($^{24}_{12}$Mg, $^{28}_{14}$Si) and heavier even-even nuclei [87] ($^{142}_{58}$Ce, $^{140}_{58}$Ce, $^{138}_{56}$Ba, $^{120}_{50}$Sn). The sought after shell-model effects on the neutron emission are suggestive, but not definitive. The zero-neutron de-excitation is found to be vanishingly small ($<2\%$) in the four heavy nuclei studied, in agreement with the general trend previously established in these type of experiments [18, 19].

In the experiments of MacDonald et al. [1] the probability for the formation of isotopes with the same mass as the capturing nucleus was found however to be high for intermediate nuclei (19% in $^{56}_{26}$Fe) and between 5–10% for heavy nuclei (except Pb for which they also found $<1\%$). It should be remarked that in the γ-ray experiments [18–20, 87] only 60–80% of the capturing processes are being accounted for. Those unaccounted for are presumably capture events in which no excited nuclei are left. It is however hard to believe that all the μ-capture events without neutron emission go directly to the ground state of the resultant nucleus – which would account for the discrepancy. One should also add that recent activation experiments by Bunatyan et al. [23, 24], in which they measure the relative probability $W_{\mu,\nu}$ for muon capture without subsequent neutron emission, tend to support the findings of MacDonald et al. [1] for intermediate nuclei. In particular, they find $W_{\mu,\nu}$ to be $16\pm3\%$ in $^{56}_{26}$Fe, $10\pm1\%$ in $^{27}_{13}$Al, $28\pm4\%$ in $^{28}_{14}$Si and $10\pm1\%$ in $^{51}_{23}$V, in fair agreement with the findings of Ref. [1].

On the other hand, activation experiments with heavy nuclei performed by the same group [88] give $W_{\mu,\nu}$ to be $9\pm1.5\%$ in ^{208}Pb and $4\pm1\%$ in $^{139}_{57}$La. At least the figure for ^{208}Pb(μ^-, ν) ^{208}Tl appears to be in disagreement with the $0\pm3\%$ result given by Kaplan et al. [1, 89] for no-neutron emission after μ-capture in natural lead.

Heusser and Kirsten [90] have recently used advanced techniques in low-level γ-ray spectrometry to perform essentially a new type of activation experiment in muon capture physics. In their experiment,

performed on Fe, Ni, Co, Mg, and Al, the yield of the radioisotopes produced after μ-capture is determined by non-destructive γ-spectrometry, without any chemical separation, the radioisotopes being identified by both their characteristic γ-rays and half-lives. For capture in Ni they are able to determine quite accurately the neutron multiplicity distribution, since most of the μ-captures lead to detectable Co radioisotopes. Thus, they account for 80% of the captures in Ni, a figure comparable with the highest detected yields with the γ de-excitation method [18–20, 85–87]. Their result for capture in the various Ni isotopes (^{58}Ni (67.9%), ^{60}Ni (26.2%), ^{62}Ni (3.2%)) compared to the calculated yields by using the model of Ref. [13] (including direct emission), is given below:

Reaction	Measured yield (%)	Calculated yield (%)	
		$M^* = 0.5\,M$	$M^* = 0.8\,M$
^{58}Ni (μ^-, ν) ^{58}Co	24.3 $\pm$2.0	19.0	22.3
^{58}Ni $(\mu^-, \nu n)$ ^{57}Co	41.3 $\pm$2.9	39.0	41.3
^{58}Ni $(\mu^-, \nu 2n)$ ^{56}Co	4.6 $\pm$0.5	13.4	8.1
^{58}Ni $(\mu^-, \nu 3n)$ ^{55}Co	0.36 $\pm$0.11	4.2	0.48
^{60}Ni (μ^-, ν) ^{60}Co	7.9 $\pm$0.6	6.1	7.6
^{62}Ni $(\mu^-, \nu n)$ ^{61}Co	2.5 $\pm$0.5	2.2	2.5
Ni $(\mu^-$, charged part.)	2.6 $\pm$0.3		
^{58}Ni $(n, 2n)$ ^{57}Ni	0.08 $\pm$0.02		
	Σ = 80.7 $\pm$3.8		

The agreement with theory for $M^* = 0.8\,M$ is, indeed, remarkable for all the measured neutron multiplicities. The unaccounted yield is estimated to be due mainly ($\sim$16%) to capture leading to the stable ^{59}Co isotope [^{60}Ni (μ^-, n) ^{59}Co] and the rest of $\sim$4% to captures leading to $^{62-64}$Co and unobserved charged particle emissions. Other interesting results of Heusser and Kirsten [90] are the yields for neutronless captures in ^{59}Co (μ^-, ν) ^{59}Fe (15.1 $\pm$ 1.1%), ^{56}Fe (μ^-, ν) ^{56}Mn (20.1 $\pm$ 1.3%) and ^{24}Mg (μ^-, ν) ^{24}Na (17.0 $\pm$ 2.6%). The latter figure appears consistent with the findings of Miller et al. [86], and the result for ^{56}Fe agrees well with measurements done with different techniques [1, 23]. On the other hand, Backenstoss et al. [18] give for neutronless capture in ^{59}Co a result which is 8 times (!) smaller than that of Heusser and Kirsten. The theoretical yields for neutronless capture calculated with Singer's model [13] for $M^* = 0.5\,M$ agree very well with the results of Heusser and Kirsten, giving 15.4% for ^{59}Co, 17.1% for ^{56}Fe and 19.2% for ^{24}Mg.

Of special interest is the role played by the giant multipole resonances in the muon capture [6–8]. One can expect that in

particular in light and intermediate nuclei, the deexcitation of the giant excited states would manifest itself in line spectra of emitted neutrons. Calculations of these spectra for several light nuclei have been performed by Überall et al. [25, 26, 27] and recently experiments have reported the observation of the predicted lines superimposed on the evaporation spectrum. Evseev et al. [9, 28] reported this effect for ^{16}O, ^{32}S, and ^{40}Ca and Plett and Sobottka [29] for ^{12}C and ^{16}O.

Temple et al. [85] probe the resonance μ-capture mechanism by comparing the relative probability of exciting various states in the resultant nucleus, with the state populations obtained in other reactions like photo and electro-excitation. Thus, they compare ^{40}Ca $(\mu^-, \nu n\gamma)$ ^{39}K with $^{40}Ca(\gamma, p\gamma')$ ^{39}K and they find that, although the same states are excited in both reactions, the correlation between the state populations is not very strong. Still, the results can be considered as evidence for the presence of the giant resonance mechanism in the μ-capture in ^{40}Ca. Likewise, they find evidence for a giant $M1$ resonance mechanism in the μ-capture process ^{28}Si $(\mu^-, \nu\gamma)$ ^{28}Al. Miller et al. [86] find good correlation for exciting the same levels in Al^{27} by the reactions ^{28}Si $(\mu^-, \nu n)$ ^{27}Al and ^{28}Si (γ, p) ^{27}Al, thus providing another evidence for a giant resonance mechanism in the μ-capture process. This topic is being analyzed in detail in Prof. Überall's talk at this Conference [81].

As the experiment indicates that the majority of the emitted neutrons in intermediate nuclei (e.g. Ca^{40}) are nevertheless of the evaporation type [5], it is of interest to calculate their emission when the excitation nuclear function is calculated by taking into account the transitions to the giant resonance states. Singer and Zin [30] have obtained the excitation function of μ-capture in Ca^{40} by using the approach of Foldy and Walecka [7] of relating the contribution to the capture probability of the giant dipole states to the appropriate photo-absorption cross section. One obtains a nuclear excitation function

$$I(Q) = A(E_m - Q)^4 \sigma_\gamma(Q)/Q + B(E_m - Q)^6 , \tag{9}$$

A, B being constants determined by the relative contribution of the dipole and the higher states to the capture probability. The multiplicity distributions calculated [30] from (9) are in good agreement with experiment [1].

2.3 Direct Neutrons and Neutron Energy Spectrum

A smaller part of the neutron emission occurs in a "direct" manner. Namely, the neutron formed in the weak process (1) succeeds in escaping from the capturing nucleus, usually with a higher energy

than the boil-off neutrons evaporated from the intermediate compound state. The direct neutrons bear information on the capture process, and the study of the spectrum of the emitted neutrons can also be a helpful tool in the understanding of the nuclear physics involved in the process. It is therefore of interest to have good data on the shape of the energy spectra of the emitted neutrons.

The earliest detailed experiment is due to Hagge [31], who measured the neutron energy spectrum between 2 and 16 MeV in calcium and lead. In this experiment the energy spectrum was measured by accumulating the pulse height spectrum resulting from neutron detection in a liquid scintillator. The spectra seem to contain a fair amount of evaporation neutrons in the low energy region. No separation or normalization to the total number of neutrons expected is made. Turner [32] has measured the energy spectra in the same nuclei in a hydrogen bubble chamber experiment. Energies of protons from neutron-proton scatterings are obtained from range relations, and then the neutron spectrum is deduced. Although neutrons with energies as high as 50 MeV are detected, only the part of the spectrum up to about 20 MeV has reasonable statistics. It appears that beyond 5 MeV the evaporation spectrum is negligible, and the percentage of

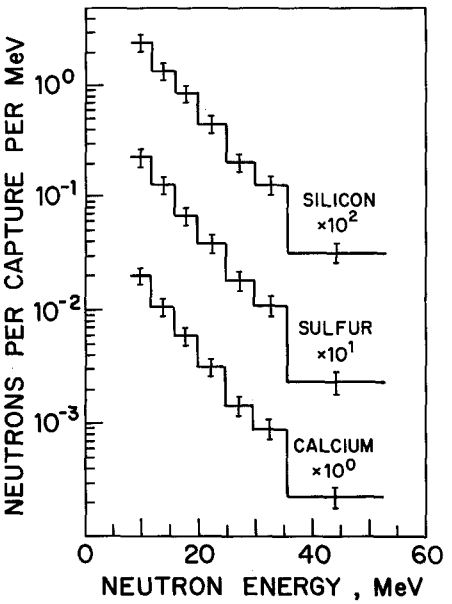

Fig. 9. Energy spectra of high energy neutrons emitted after muon capture in Si, S and Ca (Ref. [3]). These data remain essentially unchanged in the second experiment of Edelstein and Sundelin (Ref. [33])

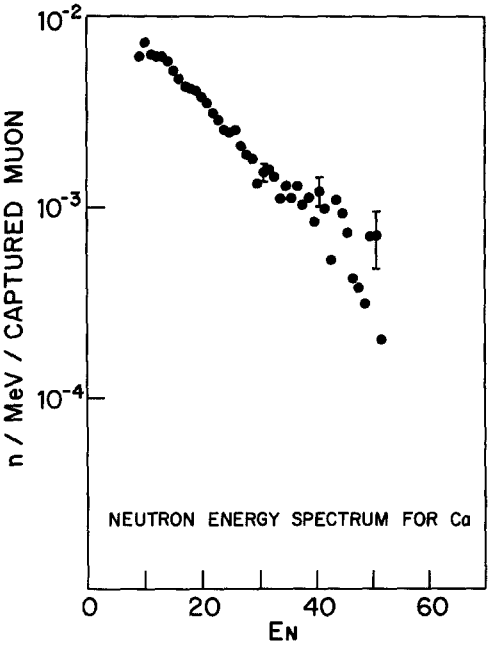

Fig. 10. Energy spectrum of high energy neutrons emitted after muon capture in Ca. (Ref. [4])

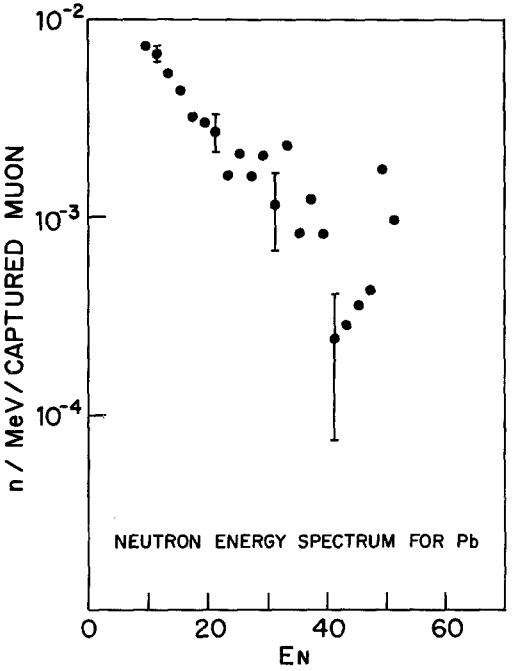

Fig. 11. Energy spectrum of high energy neutrons emitted after muon capture in Pb (Ref. [4])

directly emitted neutrons is estimated to be $20 \pm 2\%$ in calcium and $12 \pm 2\%$ in lead.

Better statistics experiments were performed recently by Krieger [4], who uses a spark chamber-scintillator neutron detector, which gives a measurement of neutron energy through the measurement of the recoiling proton in the spark chamber, and by Sundelin et al. [3, 33] who obtain the neutron spectrum by unfolding the observed pulsed-height proton spectrum. Sundelin et al. measure the spectrum in Si, S, and Ca between 7.7–52.5 MeV (Fig. 9), while Krieger gives the resulting spectrum from capture in S, Ca (Fig. 10) and Pb (Fig. 11) between 10 and 40 MeV. In both experiments one finds that the high energy neutron spectrum falls approximately in an exponential manner:

$$N(E) \sim \exp(-E/E_0). \tag{10}$$

The values obtained for the exponential constant in the two experiments are given below:

	Ref. [3]	Ref. [4]
Si	7.6	
S	7.3	15 ± 1
Ca	7.2	14 ± 1
Pb		12 ± 1

Experimental values for the constant E_0(in MeV) of Eq. (10)

Although the experiments agree on the general shape, there is clear disagreement on the value of the constant E_0.

From the experiments of Krieger [4] and Sundelin et al. [3, 33] one has also information on the percentage of direct neutrons emitted per muon capture process. Krieger [4] gives for the percentage of neutrons emitted with energies higher than 10 MeV:

$E_n > 10$ MeV	for S	0.159 ± 0.008 neutrons/μ capture
	for Ca	0.102 ± 0.005 neutrons/μ capture
	for Pb	0.091 ± 0.006 neutrons/μ capture.

The comparable figures from the experiment of Sundelin et al. [3, 33] are as follows:

$E_n > 7.73$ MeV	for Si	0.247 ± 0.044 neutrons/μ capture
	for S	0.210 ± 0.037 neutrons/μ capture
	for Ca	0.179 ± 0.031 neutrons/μ capture

$E_n > 11.49$ MeV	for Si	0.139 ± 0.025 neutrons/μ capture
	for S	0.122 ± 0.022 neutrons/μ capture
	for Ca	0.102 ± 0.018 neutrons/μ capture

In two other recent experiments measurements have been performed in the energy range of 1–15 MeV, thus covering the evaporation part as well as a portion of the high-energy part of the spectrum. Evseev et al. [9, 28] used a stilbene crystal to detect protons, and the neutron spectra from μ-capture in ^{16}O, ^{32}S, ^{40}Ca, and Pb were obtained by differentiation of proton spectra. Their results are given in Fig. 12.

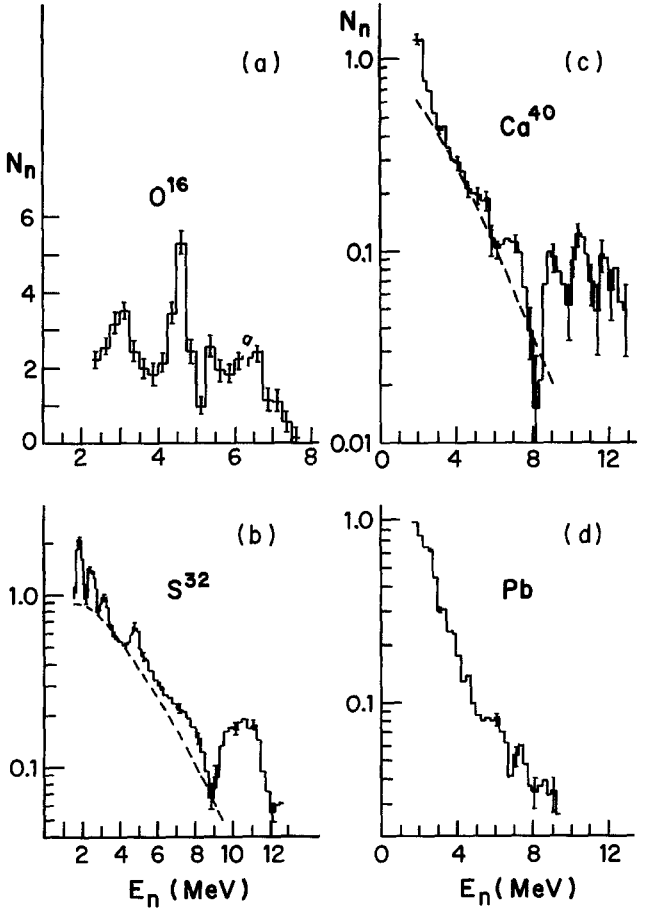

Fig. 12. Neutron energy spectra from muon capture in ^{16}O, ^{32}S, ^{40}Ca and Pb (Ref. [9])

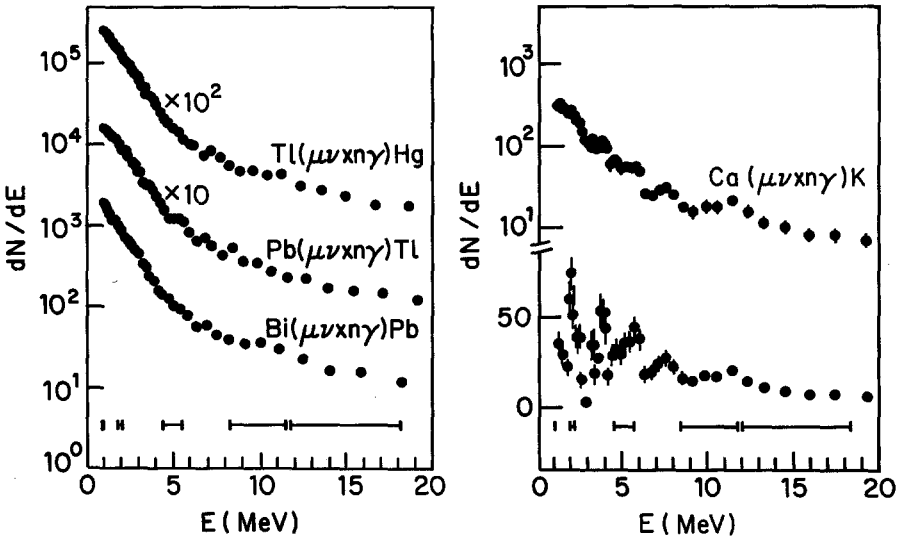

Fig. 13. Spectra of neutrons from muon capture in $_{81}$Tl, $_{82}$Pb, $_{83}$Bi and $_{20}$Ca (Ref. [5]). For capture in Ca, the total spectrum is given at the top, and that obtained after subtracting an evaporation spectrum, at the bottom

From this experiment one has evidence of line spectra in light nuclei, and characteristic lines are observed also in ^{40}Ca. The main part of the spectra in the low energy region is of evaporational type and the characteristic temperatures of the final nuclei formed after capture in S, Ca, and Pb are

$$(\theta)_S = 1.7\,\text{MeV}, \quad (\theta)_{Ca} = 1.5\,\text{MeV}, \quad (\theta)_{Pb} = 1.15\,\text{MeV}. \tag{11}$$

Schröder et al. [5] measure for the first time the spectra of neutrons from μ-capture in coincidence with de-excitation γ-rays from the resultant nucleus. The neutron energy was determined directly by using a time-of-flight method, the γ-ray serving as a signal to start the neutron measurement. The results of their measurements on neutrons in the energy range 1–20 MeV from μ-capture in Ca, Tl, Pb, and Bi are given in Fig. 13. The spectra are fitted with an evaporation-type spectrum of the form

$$dN(E) \sim E^{5/11}\, e^{-E/\theta}\, dE \tag{12}$$

in the energy range $E < 4.5$ MeV, and with an exponentially decaying form [Eq. (10)] for energies $E > 4.5$ MeV. Their results for the nuclear temperature θ, the high-energy decay constant E_0, and the percentage I of neutrons with energies larger than 4.5 MeV are given below:

Target element	θ(MeV)	E_0(MeV)	$I(E>4.5$ MeV)
$^{40}_{20}$Ca	1.35 ± 0.07	8.4 ± 1.0	$3-20\%$
$^{203,205}_{81}$Tl	1.09 ± 0.04	8.8 ± 1.1	$9.6\pm0.8\%$
$^{206,207,208}_{82}$Pb	1.22 ± 0.06	9.0 ± 1.2	$10.2\pm1.0\%$
$^{209}_{83}$Bi	1.06 ± 0.05	8.2 ± 1.2	$9.7\pm1.0\%$

The results for θ are in agreement with those of Evseev et al. [9] and the general trend for the nuclear temperature is to decrease with increasing mass number. The value of E_0 for Ca agrees with Sundelin's [3] much better than with Krieger's result. On the other hand the value for Pb is in reasonable agreement with Krieger's.

The percentage of high-energy neutrons decreases with increasing mass number in all these experiments [3, 4, 5, 9]. On the whole, there is reasonably good agreement on the percentage of direct neutrons as measured by Krieger [47] and Sundelin [3, 33], compared to the results of Schröder et al. [5]. The latter found approximately 10% of direct neutrons with energies higher than 4.5 MeV for all the heavy nuclei studied, while Krieger detected $\sim 5.5\%$ of high energy neutrons with $E>10$ MeV in Pb (normalizing to 1.7 neutrons per μ-capture). In view of the complex structure detected [5] in Calcium, a comparison with the data of Krieger and Sundelin is rather ambiguous, but it appears that at least Sundelin's figures [3, 33] for the percentage of high energy neutrons are higher than those reported in Ref. [5].

It should be remarked, however, that a comparison of the results of Schröder et al. [5] with those of other experiments [3, 4, 9, 33] has a serious limitation in the fact that the latter are able to record absolute values for the amount of neutrons detected in a certain energy range (normalized per muon capture), while the values of Ref. [5] are expressed with relation to their detected spectrum. Nevertheless, it is very interesting that, although in Ref. [5] only those neutrons which originate from excited states are detected (in coincidence with γ's), the energy spectrum is quite similar to that of the other experiments in which also transitions to ground states are detected. Thus, the above mentioned comparison is probably more meaningful than one might have expected.

Before proceeding to discuss theoretical work, it is interesting to remark that even in light nuclei there is a sizable amount of evaporation neutrons emitted after μ-capture. Plett and Sobottka [29] have found 62% of the emitted neutrons after capture in O^{16} to fit an evaporation spectrum with $\theta=1.25$ MeV, while for C^{12} the appropriate figure is 38%, with a nuclear temperature $\theta=1.01\pm0.30$ MeV.

Theoretical work on the mechanism for direct neutron emission following muon capture in intermediate and heavy nuclei has had only limited success in accounting for the observed spectrum of high energy neutrons or for the percentage of direct emission. In fact, the early calculations predicted the vanishing of the high energy neutron spectrum beyond 15–20 MeV.

Überall [34] calculated the spectrum of the directly emitted neutrons for a nucleus described by a Fermi gas model with equal numbers of protons and neutrons. Absorption or scattering of the neutrons in the nucleus is neglected. The spectrum obtained decreases linearly with energy and vanishes beyond 16 MeV. Lubkin [35] performed a "modified Fermi gas" calculation for Ca^{40} and Pb^{208}, dividing the nucleus into small boxes and treating the nucleons in each box with the Fermi gas model. The μ-capture neutron can thus be considered to appear in a localized zone of the nucleus. The thus incoherently-produced neutrons are subsequently followed out of the nucleus by geometrical optics, allowing for attenuation in the nuclear volume, and refraction and total reflection at the nuclear surface. The spectrum calculated for Ca has a peak around 5 MeV and vanishes beyond 10.77 MeV, while that for Pb peaks at 2 MeV and vanishes beyond 4.56 MeV. Dolinsky et al. [36] used the shell-model with $j-j$ coupling for Ca^{40}, and the interaction of the outgoing neutron with the nucleus is treated by using an optical potential. The spectrum obtaines peaks also around 5 MeV, and then falls approximately exponentially to zero beyond 20 MeV. The spectra obtained in Refs. [34–36] are given in Fig. 14.

Singer [13] used a simple model to roughly estimate the probability of direct emission of neutrons from the nuclear volume following μ-capture. The nucleus is taken as a constant-density sphere and the probability for direct escape p is calculated from

$$p = P \times d \tag{13}$$

where d is the average probability of a neutron created at some point in the nucleus reaching the boundary, and P the probability of its crossing the centrifugal barrier. Using

$$d = \exp\left[-0.75\, R/\lambda\right], \tag{14}$$

where λ is the mean free path in nuclear matter and

$$P(E_n) = \Sigma B_l P_l(E_n), \tag{15}$$

where B_l is the probability of occurrence of l, and $P_l(E_n)$ the escape probability of a neutron of angular momentum $l\hbar$ and energy E_n,

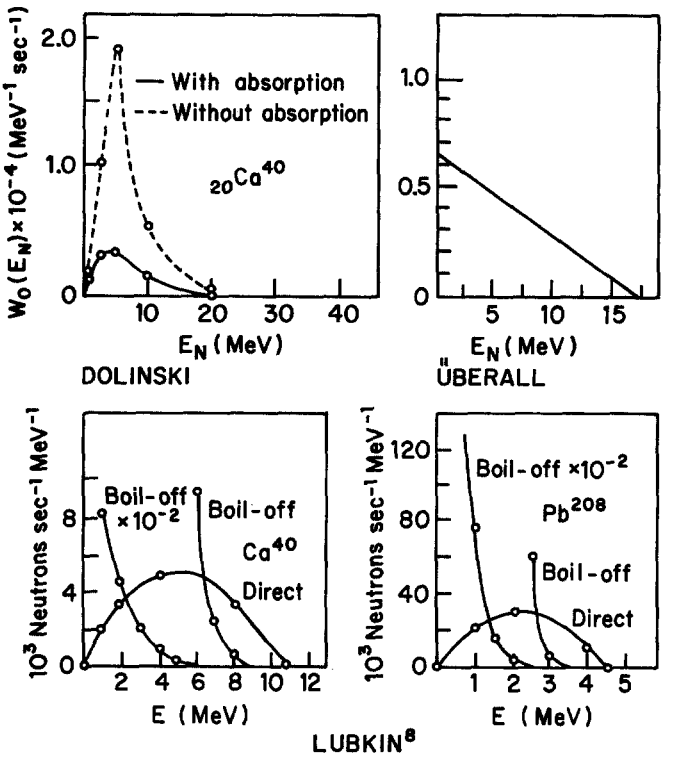

Fig. 14. Spectra for direct neutrons as calculated by Dolinsky et al. [36], Überall [34] and Lubkin [35]

one finds [13] for the percentage of direct emission in several heavy nuclei

Ag: 22%, I: 20%, Au: 16%, Pb: 15% (16)

The overall dependence on the mass number obtains correctly in this simple model. The calculation for Pb gives 9% direct neutrons out of a total average emission of 1.7 neutrons per μ-capture, in excellent agreement with Schröder's findings [5], as well as with those of Krieger [4] [5.5% direct neutrons with $E_n > 10$ MeV and remembering that the calculated figures in (16) refer to the whole spectrum of direct neutrons, i.e. $E_n \gtrsim 4$ MeV]. The constancy of the percentage of neutrons emitted directly for the three heavy elements studied by Schröder et al. [5] ($\sim 10\%$) seems to confirm the physical picture of the model of Ref. [13]. It would be interesting to have similar measurements for nuclei with $A = 100 - 120$, so as to check whether this picture still holds also for this region [from (16) one expects 15%

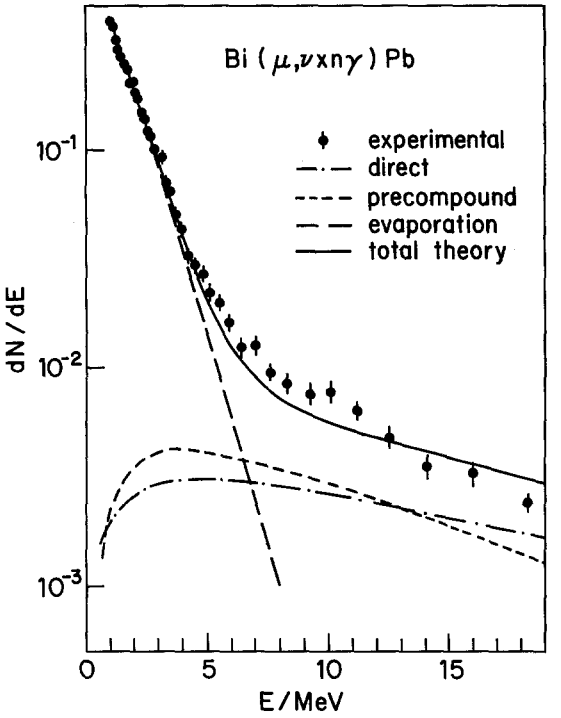

Fig. 14a. Experimental and theoretical neutron spectrum from μ-capture in Bi (Ref. [5]). The experimental spectrum is normalized to fit the theoretical one

direct neutrons out of the total average emission of ~ 1.5 per capture in this region]. The model has been refined by Schröder [5], who used it to calculate the combined evaporation and direct emission neutron energy spectrum for capture in Tl, Pb, and Bi. The agreement with the experimental spectrum of Ref. [5] is impressive, as it can be seen from Fig. 14a for capture in Bi. The direct spectrum is calculated by using a square well optical potential when following the neutron's behaviour within the nucleus. In addition, the "pre-compound" emission is also included by considering separately the neutrons which have been scattered once on other bound nucleons. The calculated integrated intensity of the direct and "pre-compound" emission amounts to 14% per capture. By adding to it a neutron evaporation spectrum for the 86% of cases of compound nucleus formation, the solid line of Fig. 14a is obtained.

Recent theoretical calculations [37, 38], which take into account relativistic effects in muon capture [39–41] as well as the interaction

between the directly emitted neutrons and the nucleus, succeed in obtaining a much more realistic spectrum of the high-energy neutrons, in fair agreement with the measurements in intermediate nuclei. Bogan [37] has calculated the energy spectrum and the asymmetry of the high-energy neutrons from μ-capture in Si, S, and Ca with the following model: (a) The effective Hamiltonian for muon capture of Fujii and Primakoff [42] is used, taking into account terms proportional to the nucleon momentum (i.e. relativistic corrections to the order of the inverse nucleon mass M^{-1} are included); (b) Harmonic-oscillator shell-model wave functions are used for the capturing proton with the harmonic-oscillator parameter chosen so as to give the proper r.m.s. charge radius; (c) Plane-waves are assumed for the emitted neutrons, their interaction with the residual nucleus being taken into account by using for the neutron momentum inside the nucleus

$$p_n^2 = 2m^* m_p(E_N + B_W) + P_F^2 , \tag{17}$$

where $m^* = 0.6\, M_N$ is the neutron effective mass, B_W the binding energy of the most weakly bound proton, and P_F the nuclear Fermi momentum. His results are compared with the experiment of Sundelin et al. [3] in Fig. 15. There is good agreement for neutron energies above 25 MeV, but the theoretical curves are a factor 2–3 lower than this experiment around 10 MeV. It should be remarked that the improved agreement with experiment is due mainly to the nuclear wave functions used and the inclusion of the final state interaction through (17). Piketty and Procureur [38] have shown by an exact treatment of the Fermi-gas model that inclusion of relativistic terms to order M^{-2} does not affect the neutron spectrum (although they do contribute appreciably to the neutron asymmetry). Moreover, they have also calculated the high energy neutron spectra from μ-capture in ^{12}C, ^{28}Si, ^{32}S, ^{40}Ca by using also realistic shell-model wave functions for the capturing proton and eikonal-type distorted wave functions for the emitted neutron in order to take into account the final state interaction. The eikonal approximation is used for neutrons with energies $E_n \geqq 25$ MeV, with optical potential parameters deduced from neutron-nucleus scattering. They conclude that the final-state interaction has a strong effect on the neutron spectrum (Fig. 16).

This conclusion is confirmed by the calculations of Bouyssy and Vinh Mau [82, 91] who are able to obtain fair agreement [91] with the neutron spectrum of Sundelin and Edelstein [3, 33] by using Hartree-Fock wave functions and an optical potential whose imaginary part has both volume and surface components. Madurga [92] has also obtained a good spectrum in a related calculation (see Fig. 16a).

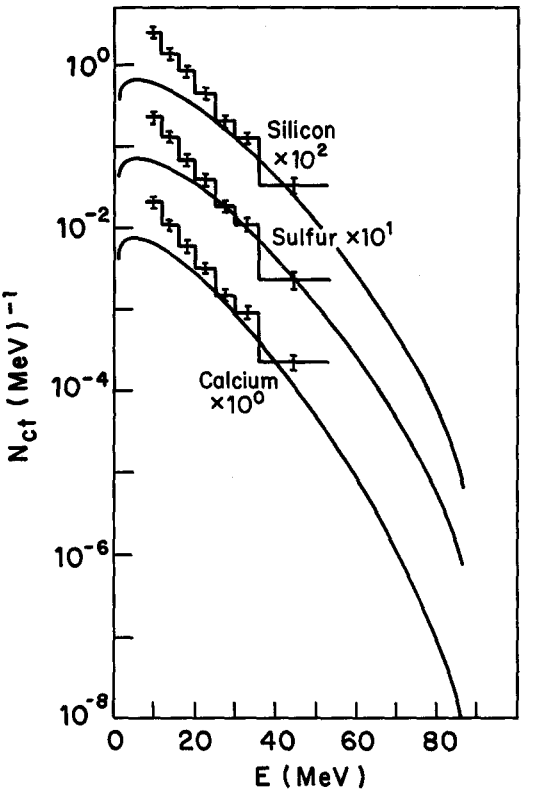

Fig. 15. Direct neutrons energy spectrum. The smooth curves are the calculation of Bogan (Ref. [37]) and the histograms are the experimental results of Sundelin et al. (Ref. [3])

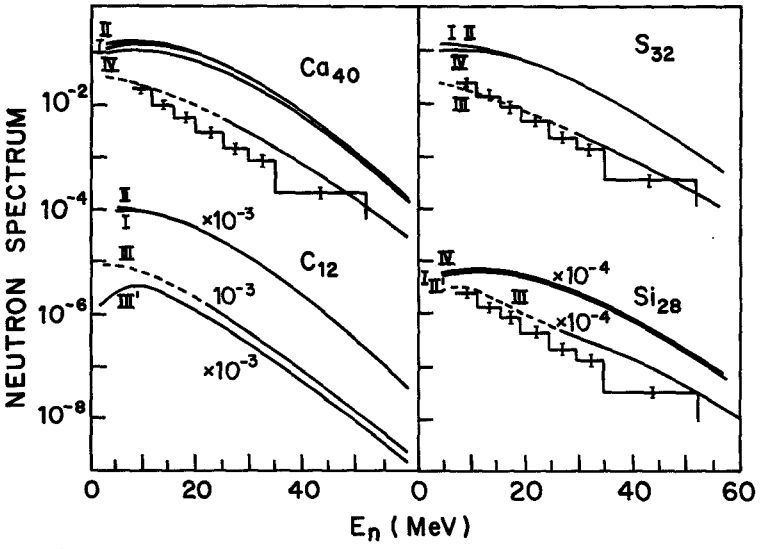

Fig. 16. Comparison of calculated neutron energy spectra by Piketty and Procureur (Ref. [38]) with the experimental results of Sundelin et al. (Ref. [3]) for Ca, S and Si

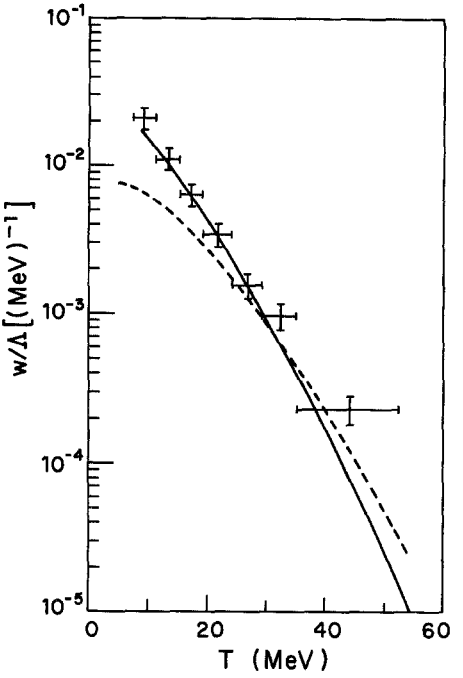

Fig. 16a. The calculation of Madurga [92] (solid line) of the neutron spectrum for Ca, compared with Bogan's calculation [37] (dashed line) and with Sundelin's data [3]

2.4 Remarks

1. From the above it appears that there is still much to be done both experimentally and theoretically on the various topics related to neutron emission following muon capture, and one hopes that the field will gain new momentum with the operation of the meson factories.

2. Although the simple calculations [1, 13] on the multiplicities of the emitted neutrons are in rough agreement with experiment, the picture is still not satisfactory. The effective mass needed to account for the average neutron emission, $M^* \simeq 0.4$–$0.5\,M$, is appreciably lower than what is considered to be the effective mass, i.e. $M^* \simeq 0.7\,M$ for $k < k_F$, from the interpretation of quasi-elastic electron-nucleus scattering experiments [43]. Improved calculations of the neutron evaporation should also take into account recent advances [44] in the knowledge of the nuclear-level densities, as the constant nuclear temperature representation appears to be valid only for the lower part of the nuclear excitation spectrum. Moreover the nuclear temperatures used in the previous calculations [1, 13] are generally lower than recently observed [5, 9].

3. There are very few attempts to account for the direct-neutrons spectrum in heavy nuclei. A calculation of the energy spectrum of direct and evaporation neutrons has been performed successfully by Schröder [5], using the simple model of Ref. [13], for the Tl, Pb, and Bi nuclei. With the advent of new experimental information, which has been accumulated in the last few years, it is high time for theorists to attack these problems, taking into account the details of nuclear structure. One would also like to have better theoretical estimates on the sensitivity of the emission processes to the nuclear models used.

4. On the experimental side, we are only at the beginning of experiments on the energy spectrum of the emitted neutrons, and there are some discrepancies between the existing experiments concerning the percentage of directly emitted neutrons. It will be of great value to have more experiments measuring *both the energy spectrum and the asymmetry of the emitted neutrons*, as well as experiments measuring *at the same time the multiplicities and the energy spectrum of the neutrons.*

5. There seems to be disagreement at present on the amount of mu-capture without neutron emission between the experiments measuring γ-rays [18, 19] and those measuring neutrons [1] or using activation methods [23, 24, 90].

III. Charged Particle Emission

3.1 General

The deexcitation of the nucleus by charged particle emission after muon capture is a very infrequent process in intermediate and heavy nuclei. Although very little experimental work has been done in this field (and likewise, hardly a matching amount of theoretical work), there is agreement on the scarcity of charged events between the pioneering extensive emulsion experiment of Morinaga and Fry [45] and the later experiments [46–48] of this type.

Morinaga and Fry [45] studied 24000 meson tracks which stopped in their emulsion. They found that the meson capture in the heavy element of the emulsion (Ag, Br) is accompanied in 2.2% of the cases by one proton emission and in 0.5% by alpha particle emission. The energy distributions of these charged particles were also obtained in the experiment and are given in Fig. 17. In a subsequent emulsion experiment [50], with nearly 4 times more statistics, Kotelchuk and Tyler [51] measured a proton energy spectrum in fair agreement with Morinaga and Fry (Fig. 18). It should be remarked that the proton spectrum of Morinaga and Fry [45] is not very accurate for energies

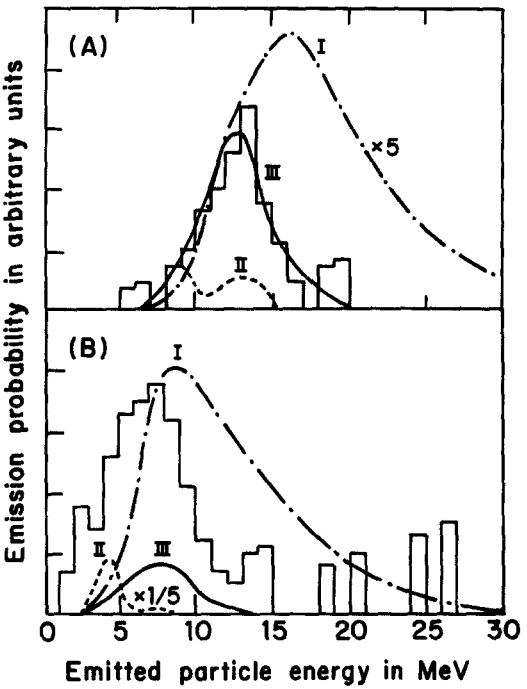

Fig. 17. Energy distribution of emitted alpha particles (A) and protons (B) following muon absorption in AgBr from the experiment of Ref. [45]. The curves are theoretical calculations of Ishii [49]

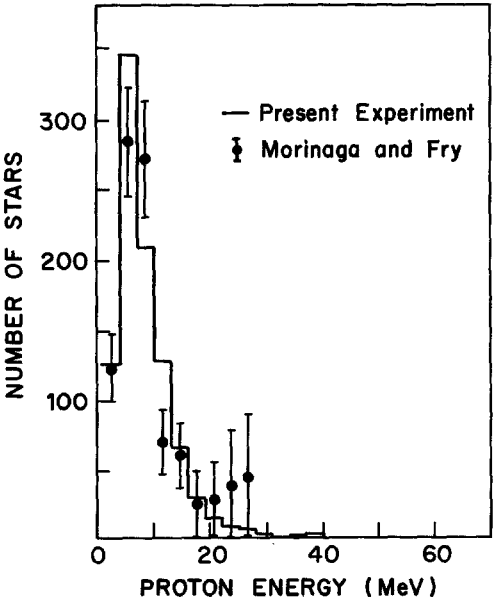

Fig. 18. Energy distribution of protons following muon capture in AgBr from the experiment of Ref. [51], compared with the earlier results of Morinaga and Fry [45]

> 15 MeV because of limited statistics and the need for large geometrical corrections.

Ishii [49] calculated the emission of protons and α-particles, assuming the formation of a compound nucleus following the μ-capture and subsequent statistical emission of various particles. He used for the nuclear level densities parameters determined from nuclear reactions at appropriate excitation energies. For the momentum distribution of protons in the nucleus he used three possible densities: (a) Fermi gas at zero temperature; (b) Fermi gas at a finite temperature ($kT = 9$ MeV) (c) The Chew-Goldberger distribution $\varrho(p) \sim A/(B^2 + p^2)^2$, which is known however from independent experiments to contain an inadequately high proportion of high momenta. Very good agreement with experiment for the α-emission is obtained with distribution (b), for both the absolute percentage (0.45% versus the experimental 0.5%) and the energy distribution (see curve *III* in Fig. 17(A)). The calculated emission of protons for the same finite temperature Fermi gas distribution turns out to be 10 times smaller than experiment. It is relevant that the distribution which accounts well for α-emission is quite similar to the one giving fair agreement [1, 13] with the experimentally observed neutron evaporation. Ishii also finds that (the unlikely) distribution (c) could account for the proton emission; however then the calculated α-emission is 15 times larger than observed.

In interpreting the results of Ishii's calculations one should also remember that at similar excitation energies the statistical theory explains satisfactorily α-emission in nuclear processes. On the other hand, under similar conditions the proton emission is frequently one to two orders of magnitude higher than that calculated from a compound nucleus with statistical emission [52, 53].

Assuming a reduced effective mass for the muon-absorbing nucleon the average calculated excitation energy available in the compound state will be increased. However, as charged particle emission takes place primarily from the momentum region near the Fermi level, and the effective-mass in this region is $M^*(p) \simeq M$, the inclusion of the effective-mass approximation does not significantly increase the calculated rate of proton emission. It appears therefore that the rate of proton emission following muon capture in Ag, Br significantly exceeds the number predicted by evaporation theory. Moreover, the observation of high energy protons with energies of 25–50 MeV also cannot be reconciled with the evaporation mechanism.

In view of the inability to account for the emission of protons as a statistical process, other mechanisms involving "direct" emission have been considered. Two models have been developed, which take into

account the two-nucleon correlation, on the surface [16] as well as in the nuclear volume [54]. They are presented in the next sections.

3.2 Surface Correlation Effects (Pseudodeuteron Model)

There is experimental evidence [55] from various nuclear phenomena (including K^--capture), that the nuclear surface is relatively rich in nucleon clusters. Theoretical calculations [56, 57] account for the clustering tendency near the surface, from the behavior as a function of distance from the center of the nucleus of the correlation-free potential energy density versus the part of it that includes correlations.

Singer [16] has suggested that capture by two-nucleon clusters in the surface region can provide the mechanism for the emission of protons unaccounted for by the statistical calculations [49]. The elementary capture process in this case would be

$$\mu^- + 2N \rightarrow 2N' + \nu_\mu . \tag{18}$$

Capture by a two-proton cluster then results in the appearance of an energetic neutron-proton pair, with a fair chance of direct escape from the nucleus. This type of process will also contribute to direct one and two-neutron emission when the capture occurs on neutron-proton pairs and it has been shown [1, 13] that it does indeed improve the agreement with experiment of calculated neutron emission.

A pseudodeuteron-model calculation has been made by Singer [16] for Ag, Br nuclei, for which experimental findings [45–48] and statistical emission calculations [49] are available. It is assumed that the effective nucleon clusters are those in the classical forbidden region, which extends beyond the radius R_c at which the sum of the nuclear and Coulomb potential vanish. Using the charge distribution in nuclei obtained from high-energy electron-nucleus scattering, one has on the average 1.5 protons in that region in Ag, Br. Only pseudodeuterons in S-states are considered, which limits the proton-proton cluster to singlet-spin state. The capture probability from a proton cluster in Ag is then shown to be related [16] to the capture probability from a deuteron [58] ω_D by

$$\omega_{[p-p]0} = 1.74\,\omega_D \frac{|\phi_\mu, \mathrm{Ag}(R_c)|^2}{|\phi_{\mu,D}(0)|^2} \frac{2\pi\,(1-\bar{\alpha}r_0)}{\bar{\alpha}\langle\alpha^2+k^2\rangle v} . \tag{19}$$

The differences between ω_D and $\omega_{[p-p]0}$ are due to: (1) different spatial wave functions, which can be compensated for by taking into account the ratio of normalization constants of the two wave functions [last factor in (19)]; (2) a different value for the muon wave function in the

capture region; (3) the allowed final states [included in the numerical factor in (19)]. Assuming that half the protons produced after muon capture by a pseudodeuteron leave the nucleus, and that S-wave singlet proton-pairs in the nuclear surface behave 40% of the time [59] as pseudodeuterons, Singer finds [16] that 0.022 protons are emitted per μ-capture in Ag and Br. Keeping in mind that some of the figures used are uncertain (like the 40% clustering probability, the 50% probability for escape, the exact form of the pseudodeuteron wave function), the perfect agreement with the experiment of Morinaga and Fry [45] is to some extent fortuituous.

In the above calculation no energy spectrum for the emitted protons is deduced. The kinematics of the reaction however allows for the appearance of energetic proton from pseudodeuteron capture with energies up to $E_{max} \simeq 50$ MeV. Such energetic protons, unaccounted for by evaporation, have indeed been observed [48, 51]. The peak of the spectrum on the other hand is expected to be below 10 MeV.

3.3 Volume Correlation Effects

Accepting the result of Ishii [49] that the evaporated protons following muon capture in Ag and Br can account for only 10% of the proton emission, one has still to check whether some form of direct emission from the nuclear volume might possibly account for the observed rate. One can think of a direct process initiated by the neutron created in the weak-interaction process (1). The neutron could possibly knock out of the nucleus a proton on which it scatters. The direct "knock-on" mechanism for (p, p') reactions has been studied for nuclear reactions, where the inelastic scattering cross sections for protons with a few tenths of MeV are larger by order of magnitude than calculated by statistical process. Elton and Gomes [60] have shown however that the total reflection at the nuclear boundary essentially prevents these protons from directly leaking outside and the contemplated "knock-on" direct emission from the nuclear volume is even smaller than the compound nucleus emission. Hence the direct emission of protons from the nuclear volume following μ-capture appears to be very improbable in view of the results of Elton and Gomes [60]. It should be added that the large cross-sections for (p, p') reactions are accounted for by considering quasi-elastic scatterings taking place mainly in the nuclear surface [53, 60, 61].

Bertero, Passatore, and Viano [54] have considered another possibility for direct emission from the nuclear volume, taking into account nuclear correlations. In particular, they consider the possibility

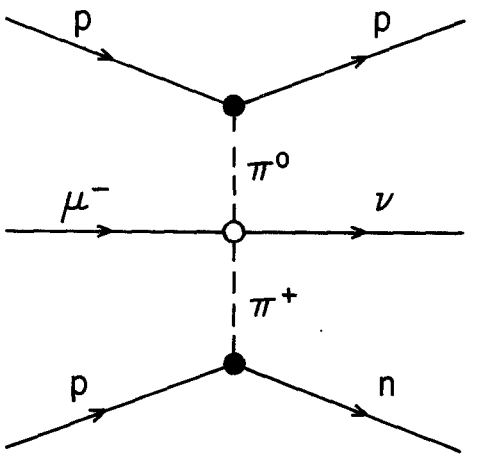

Fig. 19. The Feynman diagram for μ-capture by proton pairs considered by Bertero, Passatore and Viano [54]

of μ-capture by proton pairs, the weak ($\mu\nu$)-current interacting directly with the pion current exchanged by the nucleon pair. The Feynman diagram considered in their paper is exhibited in Fig. 19. The strength of the weak vertex involved is known (up to a form factor) from the β-decay of the pion which agrees with the prediction of the CVC theory. They calculate the diagram from the following interaction Hamiltonian

$$H_{\text{int}} = ig(\bar{\psi}_N \gamma_5 \tau_i \phi_i \psi_N) + 2^{-1/2} G (\bar{\psi}_\nu \gamma_\sigma (1+\gamma_5)\psi_\mu)(\varepsilon_{1jk} - i\varepsilon_{2jk}) \cdot (\phi_j \partial_\sigma \phi_k)$$

where g is the renormalized pion-nucleon coupling constant and G, the weak vector-coupling constant. In the calculation of the matrix elements the static limit is used for nucleons which are then treated as a Fermi gas, and closure approximation is used in calculating the capture probability.

It is then assumed that a proton produced anywhere in the nucleus always arrives at the nuclear surface and the probability of its being transmitted through the nuclear surface is estimated by using transmission functions [62]. One obtains a proton emission rate of 1.7% for Ca^{40}, 1.2% for Ag^{107}, and 1.1% for ^{208}Pb. The energy spectrum calculated for capture in ^{107}Ag shows a peak around 25 MeV and extends up to proton energies of 80 MeV.

In the calculation of Bertero et al. [54] a particular diagram was singled out. However, to the same order in the interactions considered there are additional diagrams contributing to the process, which could interfere destructively with the one taken into account [63]. In fact, one

knows that as a consequence of Siegert's theorem [64, 65] on the interaction between nucleons and the radiation field, there are no exchange terms contributing to the electric multipole transitions, and in the limit of zero photon energy they completely disappear due to the vanishing of the magnetic terms. Experimentally this result seems to hold also for fairly high ($\lesssim 100$ MeV) photon energies. On the basis of CVC theory, one expects an extended Siegert theorem to hold also for the vector part of the weak interaction [66]. Hence, the exchange contribution might be much smaller than calculated by Bertero et al. [54]. This has been recently verified experimentally by Kotelchuk and Tyler [51] as discussed in the following section.

3.4 Recent Experiments

In the last few years several new experiments on the detection of charged particles following muon capture have been performed.

Kotelchuk [46] analyzed an emulsion experiment [50] containing nearly 10^5 muon endings. He found evidence for muon capture in the nuclear surface [16] from the number of one-prong stars found, their expected number for surface or volume capture being deduced from neutron reactions at comparable energies. In a subsequent analysis [51] of the same plates, Kotelchuk and Tyler present convincing evidence against the preponderance of the mechanism of capture by exchange currents suggested by Bertero et al. [54]. The proton-energy spectrum, obtained from 1289 single-prong μ-stars, peaks at 7–8 MeV, as opposed to the peaking around 25 MeV predicted by Bertero et al. (Fig. 20). Also, much fewer protons than predicted are observed in the 20–40 MeV region, and there is complete absence of stars beyond 40 MeV, while more than 100 were to be found from the mechanism of Bertero et al. [54]. Kotelchuk and Tyler then conclude that this mechanism occurs less often than predicted at least by a factor $(2.0 \pm 1.0) \times 10^{-2}$. On the other side, the experimental spectrum is quite consistent with Singer's pseudodeuteron model [16].

Vaisenberg et al. [47], from an emulsion experiment, report 3% probability for charged particle emission following μ-capture, in agreement with previous results. In a high-statistics emulsion experiment involving $(2.74 \pm 0.14) \times 10^5$ stopped muons, Vaisenberg et al. [48] investigate the spectrum of protons with energies higher than 25 MeV (they have 87 events in this region). Their results agree very well, within the statistical accuracy, with Kotelchuk and Tyler on the fraction of protons with energies higher than 25 MeV emitted per muon capture, which is found to be $3.16 \pm 0.34 \times 10^{-4}$. However,

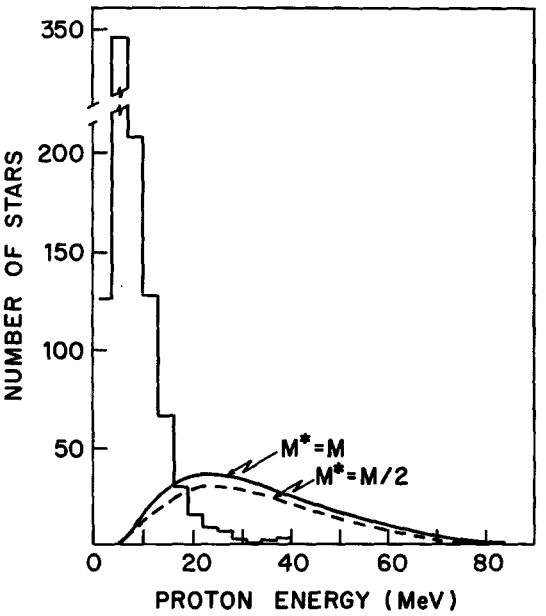

Fig. 20. Comparison of the experimental [51] proton energy spectrum with the predictions of Bertero et al. [54] (solid and dotted curves). The histogram represents the data corrected for α-particle emission and stars off light nuclei

they also find 13 events with protons having energies which extend up to ~ 80 MeV, amounting to $(4.7 \pm 1.1) \times 10^{-5}$ protons per capture, with energies beyond 40 MeV. They estimate that the possible admixture of pion stars in this energy region does not exceed 30%; hence this cannot explain away these high energy events. If it is then assumed that all the protons detected as having energies beyond 25 MeV are due to the Bertero mechanism [54], the latter will then account for only $\sim 2\%$ of the observed total proton emission. This agrees with the previous observation of Kotelchuk and Tyler [51] on the very small frequency of this mechanism.

So far we have discussed proton emission from the heavy nuclei of the nuclear emulsion. From these experiments there are also results on the percentage of charged particle emission per mu-capture from the light nuclei of the emulsion, namely C, N, and O. Morinaga and Fry have found [45] that, of muon capture in these light nuclei, 9.5% results in proton emission, and 3.4% in alpha emission. Vaisenberg et al. [47] confirm that the probability of emission of at least one charged particle after μ-capture in the light emulsion nuclei is $\sim 15\%$.

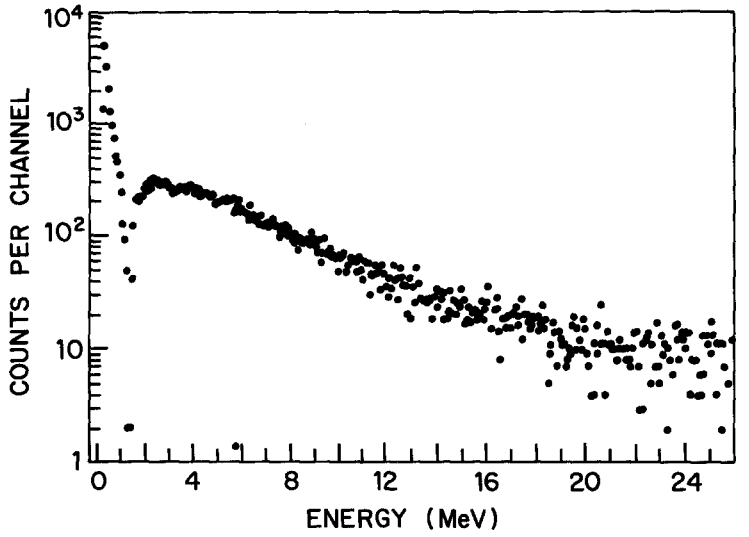

Fig. 21. The corrected energy spectrum for charged particle (supposedly mainly protons) emission following mu-capture in Si^{28} (Ref. [67])

Komarov and Savchenko [93], in a liquid-hydrogen with additions of neon bubble-chamber experiment, detect the charged particle emission following muon capture in another light nucleus, Neon, to be as high as $20 \pm 4\%$.

Sobottka and Wills [67] have performed a pioneering high-resolution experiment, in which the charged particles emitted after mu-capture in Si^{28} are detected by a Si(Li) scintillator. The spectrum of the charged particle emission, corrected for electron background and escape of protons, is given in Fig. 21. The low-energy end of the spectrum is identified as due to the Al^{27} recoiling nuclei from the $\mu^- + Si^{28} \rightarrow Al^{27} + n + \nu_\mu$ reaction, while the rest should be mainly due to the protons from $\mu^- + Si^{28} \rightarrow Mg^{27} + p + \nu_\mu$. There is however, no separation from other possible charged particles like α and d, which can be emitted by the excited Al^{28} nucleus. It should also be kept in mind that the protons can also come from $\mu^- + Si^{28} \rightarrow Mg^{26} + p + n + \nu_\mu$. The spectrum attributed by the authors mainly to protons (Fig. 21) has a low-energy cutoff at 1.4 MeV and a maximum at about 2.5 MeV, from which it decreases approximately exponentially with a decay constant of 4.6 MeV. The spectral integral gives 15% charged particle emission per mu-capture in Si^{28}. The figure is slightly higher than that obtained in emulsion experiments [45, 47] from the light C, O, N nuclei, but compares favourably with Komarov's [93] figure on Neon.

Vil'gel'mova et al. [68] have used an activation method to measure the probabilities of single proton emission after mu-capture in Si^{28} and K^{39}. In their experiment the final nucleus is identified from its radioactivity, their method thus providing a direct measurement for the $Si^{28}(\mu^-, p\nu_\mu)Mg^{27}$ and $K^{39}(\mu^-, p\nu_\mu)Cl^{38}$ reactions, which was not possible in the experiment of Sobottka and Wills [67]. They obtain for the percentage of single proton (unaccompanied by neutron) emission

$$W_{\mu^-, p\nu_\mu}(Si^{28}) = 5.3 \pm 1.0\%, \quad W_{\mu^-, p\nu_\mu}(K^{39}) = 3.2 \pm 0.6\%. \tag{20}$$

If the results of Refs. [67] and [68] are sufficiently accurate, an interesting conclusion is that the reaction $Si^{28}(\mu^-, pn\nu_\mu)Mg^{26}$ is probably as frequent as $Si^{28}(\mu^-, p\nu_\mu)Mg^{27}$ and moreover, the 15% charged particle emission measured by Sobottka and Wills [67] probably contains a fair percentage of α and d.

As mentioned in Section 2.2, the Russian group had previously measured [24] the $Si^{28}(\mu^-, \nu_\mu)Al^{28}$ reaction, for which they found a $28 \pm 4\%$ probability. Thus, the combined results for (μ^-, ν_μ) and $(\mu^-, p\nu_\mu)$ of the Russian group give $33 \pm 4\%$ probability for muon capture in Si^{28} without subsequent emission of neutrons. This agrees very well with the figure of $36 \pm 6\%$ for no-neutron emission obtained by MacDonald et al. [1, 69].

Qualitative confirmation of these results on proton emission, following μ-capture in Si^{28} is presented by Miller et al. [86] and by Temple et al. [85], who used the delayed $-\gamma$ method to identify the nature of the emitted particles. Temple et al. [85] have also evidence for charged particles emission after capture in Ca.

Budyashov et al. [70] have recently performed a counter experiment to study the charged particles following muon capture in several light and intermediate nuclei, with the specific aims of separating the charged particles by masses and measuring the energy spectra of the emitted protons, deuterons and tritons. The targets used in the experiment were ^{28}Si, ^{32}S, ^{40}Ca, and ^{64}Cu. The proton energy spectra are measured from $E_p = 15$ MeV and extend to ~ 60 MeV and those for deuterons are measured from $E_d = 18$ MeV and extend to ~ 50 MeV (Fig. 22). The yield of proton emission with energies above 15 MeV was found to be $0.88 \pm 0.06\%$ for ^{28}Si, $1.30 \pm 0.11\%$ for ^{40}Ca and $0.60 \pm 0.07\%$ for ^{64}Cu. The yield of deuteron emission with energies above 18 MeV obtains as $0.33 \pm 0.03\%$ for ^{28}Si, $0.22 \pm 0.03\%$ for ^{40}Ca and $0.10 \pm 0.03\%$ for ^{64}Cu. Their detailed results are presented in Figs. 23, 24. The amount of tritium was found to be much smaller. The decrease in the percentage of deuteron emission from the total yield of charged particles with the increase of the charge number

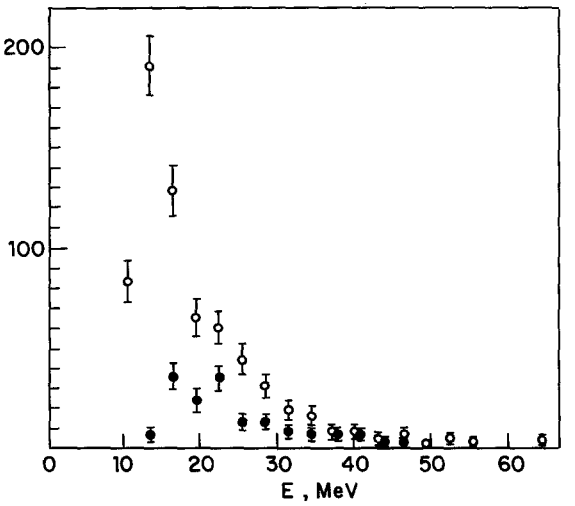

Fig. 22. The energy spectra of protons (○) and deuterons (●) from mu-capture in ^{32}S (Ref. [70])

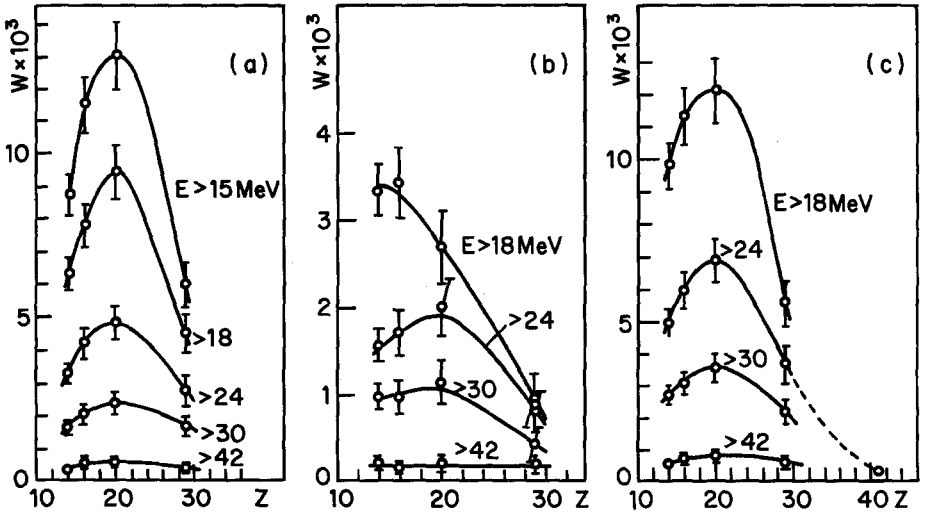

Fig. 23. Dependence of the integral probability of charged particle emission on the nuclear charge, from the experiment of Ref. [70] for (a) protons, (b) deuterons, (c) total charged particles

agrees with an earlier estimate from emulsion experiment [47]. The ratio of deuteron to proton emission found in this experiment should be of great value to the theoretical formulation of charged particle emission in these nuclei.

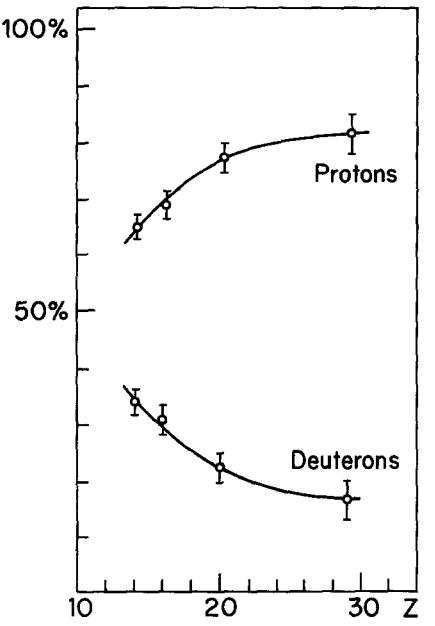

Fig. 24. Proton and deuteron yields as fractions of the total charged particle emission, for several nuclei (Ref. [70])

Before concluding, we should like to add that the scarcity of proton emission in heavy nuclei has been confirmed also in the experiments of Backenstoss et al. [18] and Petitjean et al. [19], who find respectively less than 1% and 3% possible proton emission in the nuclei studied.

Furthermore, Heusser and Kirsten [90] conclude from their activation experiment that the charged particle emission following μ-capture in Ni is $\sim 4\%$, while Miller et al. [87] find no evidence whatsoever for charged particle emission following μ-capture in ^{142}Ce, ^{140}Ce, ^{138}Ba, and ^{120}Sn.

3.5 Remarks

1. There is hardly any need to emphasize the lack of detailed theoretical attempts to treat the problem of charged particle emission from nuclei following mu-capture. With the experimental information which has been accumulating in the last few years, there is more ground now for testing possible theoretical approaches.

2. The existing experimental evidence [48, 51] appears to rule out the exchange current mechanism [54, 63] as the main contribution to the rate of proton emission from heavy nuclei.

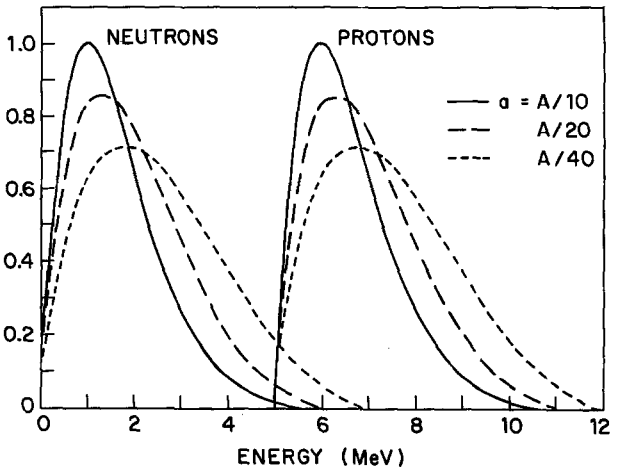

Fig. 25. Calculated evaporation spectra of neutrons and protons from Ge^{68} at 20 MeV excitation energies (Refs. [53, 71])

3. The rate and the energy spectrum of the protons emitted after mu-capture in Ag, Br are in qualitative agreement [46–48, 51] with the pseudodeuteron model [16]. There is however no detailed prediction available of this model concerning the expected energy spectrum. Nevertheless, it should be remarked that the high energy protons (up to 80 MeV) observed by Vaisenberg et al. [48] are not unaccounted for in the pseudodeuteron model. The maximal energy of 50 MeV protons expected from the model is only a first approximation, as the motion of the pseudodeuterons in the nuclear surface would certainly smear out the 50 MeV limit.

4. It would be of great interest to measure the asymmetry of the emitted protons with respect to the muon polarization. Such an asymmetry would single out the pseudodeuteron model (or some other yet unthought of form of direct emission) versus the symmetric distribution expected for evaporation protons.

5. The calculation of Ishii [49] excludes the evaporation mechanism as the main producer of protons following mu-capture in Ag, Br. The observed spectra of the protons [45, 48, 51, 70] are also indicative of a direct mechanism, particularly in view of the amount of relatively high energy protons observed.

For comparison one can look at nuclear reactions at the appropriate energies. In Fig. 25 we show the calculated [53, 71] evaporation spectra of neutrons and protons from Ge^{68} at 20 MeV excitation energies, the average excitation energy in intermediate and heavy nuclei after mu-capture being also 15–20 MeV. The neutron evapora-

tion spectrum observed [5, 9] after mu-capture is similar to that in Fig. 25 while that observed for protons [45, 48, 52] definitely shifts towards higher energies. The evaporation spectra of protons from nuclear reactions at excitation energies of 15–20 MeV do follow [53, 71] the general shape of Fig. 25, with a maximum between 3–5 MeV.

It is nevertheless of interest to have additional calculations on the contribution of evaporation to the spectra of charged particles in various nuclei, as its contribution might still be sizable in certain nuclei, at least for the lower energy part of the spectrum.

IV. Neutron and γ Asymmetry

The angular distribution of direct neutrons emitted following muon capture in nuclei is expected to exhibit an asymmetry with respect to the direction of polarization of the captured muons. The asymmetry, related to parity violation in weak interactions carries information on the weak interaction coupling constants. Likewise, the γ-rays from radiative muon capture exhibit an angular asymmetry with respect to the μ-polarization. As these topics have also been discussed at this Conference by Prof. Überall and Dr. Rosenstein, we shall record here only briefly some recent developments on these topics.

The angular asymmetry of the neutrons can be expressed [72]

$$F(\theta) = 1 + P_\mu \alpha(E_n)\, \theta_{\mu n}\,. \tag{21}$$

P_μ is the degree of muon polarization, and $\alpha(E_n)$ contains both nuclear and weak-interaction information. In simple models one can separate $\alpha = \alpha_C \cdot \alpha_N$, where α_N contains the nuclear matrix elements, and α_C contains only the weak interaction coupling constants. Primakoff's [73] formula for α_C in spin-0 nuclei gives

$$\alpha_C = \frac{G_V^2 - G_A^2 - 2\,G_A\,G_P + G_P^2}{G_V^2 + 3\,G_A^2 + G_P^2 < 2\,G_A\,G_P} \simeq -0.4\,. \tag{22}$$

The inclusion of momentum dependent terms has been shown [39] to increase α_C to -0.11. α_N depends fairly strongly on E_n and its calculation, resulting in values between $0.2-0.8$, is quite model-dependent [72].

Early measurements [74] of α in Ca and Si indicated negative values close to -1. A more recent experiment by Sculli [75] shows the possibility of positive α in Ca (Fig. 26). Sundelin et al. [76, 33] have recently measured the asymmetry parameter for capture in Si, S, and Ca, for neutron energies ranging between 10 and 45 MeV. They obtain for all nuclei studied positive values for α which generally increase with neutron energy (Figs. 27–31).

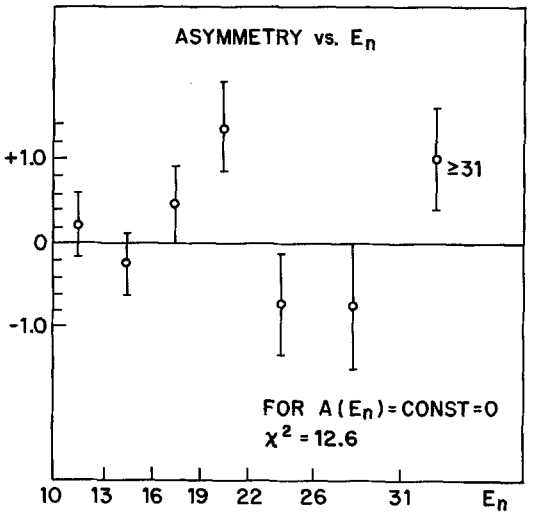

Fig. 26. The neutron asymmetry as a function of neutron energy from mu-capture in Ca^{40} (Ref. [75])

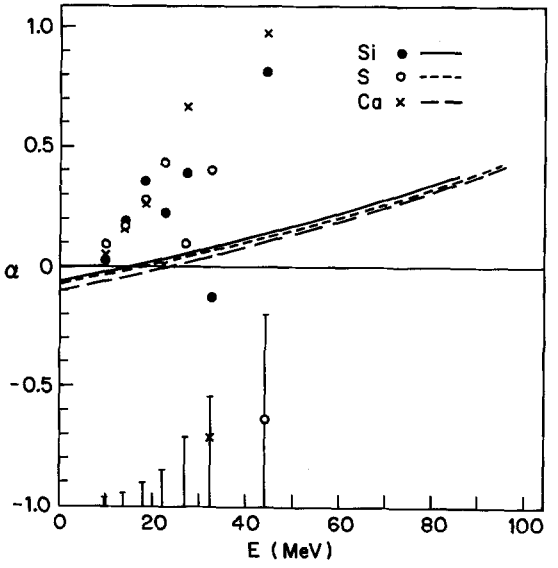

Fig. 27. Calculation of Bogan [37] of the neutron asymmetry coefficient compared to the measurements of Sundelin et al. [76]. The standard deviation of the experimental data is shown at the bottom of the figure

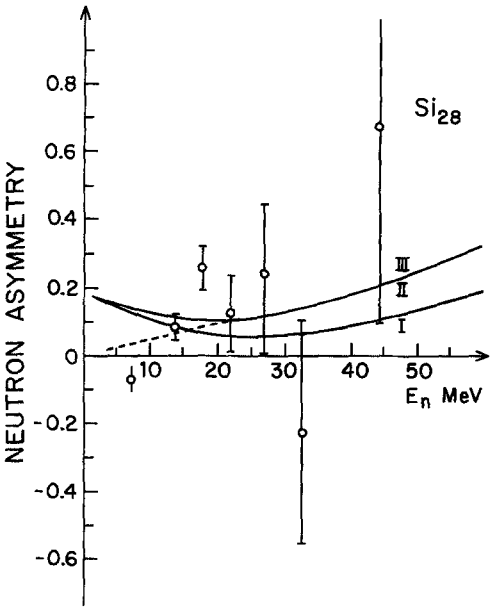

Fig. 28. Calculations [38] of the neutron asymmetry coefficient in Si^{28} compared to Sundelin's measurement [76]

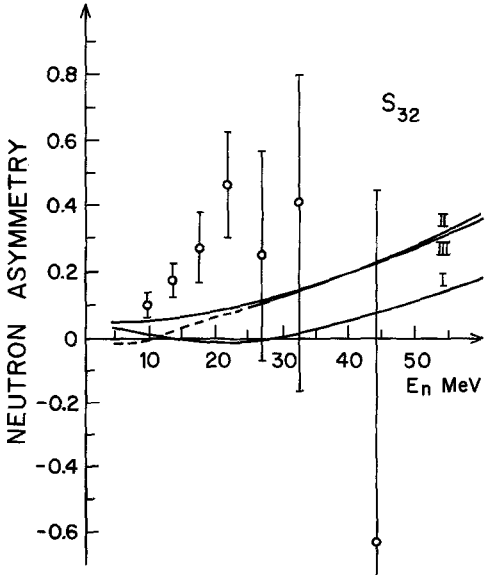

Fig. 29. Calculations [38] of the neutron asymmetry coefficient in S^{32} compared to Sundelin's measurement [76]

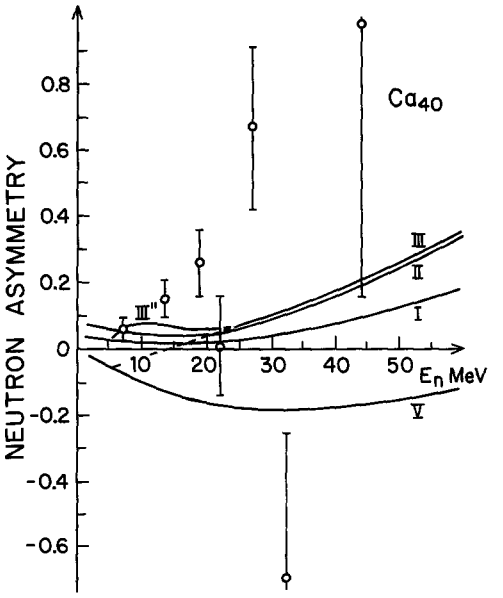

Fig. 30. Calculations [38] of the neutron asymmetry parameter in Ca^{40} compared to Sundelin's measurement [76]

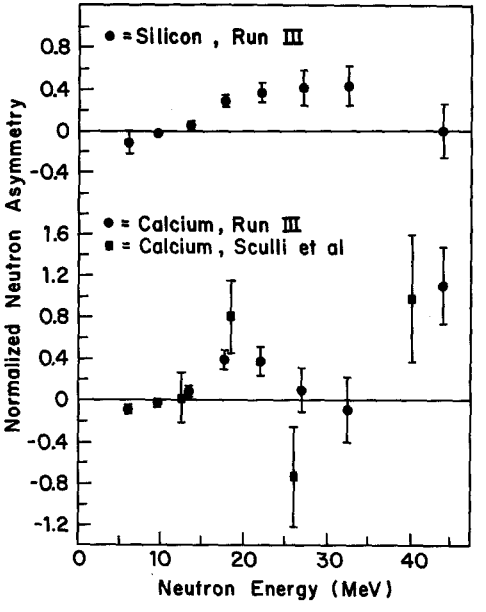

Fig. 31. The neutron asymmetry parameter for Si and Ca from the second experiment of Edelstein and Sundelin (Ref. [33])

In Figs. 27–30 some theoretical calculations are compared with the older data [76] of Edelstein and Sundelin, while in Fig. 31 their new data (the second of Ref. [33]) are presented. There is general agreement between the two sets of data, the newer experiment [33] enjoying, however, much better statistics. The later experiment also gives additional evidence to the apparent energy variation of α, which seems to reach maximal positive values of ~ 0.4 for both Si and Ca around 20–30 MeV, then possibly decreasing for higher energies.

Also, in a new experiment [94], Evseev's group has remeasured the polarization coefficients in Calcium and Sulphure. Their new values are $\alpha_{Ca} = 0.035 \pm 0.11$ (average over the energy range $2\,\text{MeV} < E_n < 17\,\text{MeV}$) and $\alpha_S = 0.015 \pm 0.025$ (average over the energy range $2.5\,\text{MeV} < E_n < 10\,\text{MeV}$). These values are not in disagreement any more with the results of Edelstein and Sundelin [33, 76] in these energy ranges.

Positive values for α were unexpected from earlier estimates [39]. However, recent calculations by Bogan [37] and Piketty and Procureur [38], who include relativistic effects up to order $1/M$ [37] and $1/M^2$ [38] in their shell model treatment of the process, show that positive α's are thus obtainable [82]. Their results (Figs. 27–30), although in the right direction, are generally smaller than Sundelin's [33, 76] values.

A comparative analysis of the recent theoretical papers [37–39, 80, 82, 95–97] dealing with the neutron asymetry, leads to certain conclusions on the importance of the various factors entering the calculation of α. Thus, there is general agreement [37–39, 96] that the inclusion of relativistic effects, as suggested firstly by Klein, Neal and Wolfenstein [39] will increase the value of α in the direction of positive values. Keeping terms up to order P_n/M (first-order relativistic correction) in a Fermi-gas model calculation of α, the authors of Ref. [39] obtained values which are less negative than in the non-relativistic case. Piketty and Procureur [38] have shown that additional improvement is obtained by also including contributions to order M^{-2}, although the values are still slightly negative for neutron energies $E_n > 5\,\text{MeV}$, while a fully relativistic Fermi-gas treatment does not bring any further changes. Nevertheless, by assuming effective masses $M_p^* = M_n^* = M/2$ one can push α to small positive values. For ^{40}Ca, α then changes [96] between 0.05 and 0.02, for E_n varying between 0 and 30 MeV.

Bogan [37] and Piketty and Procureur [38] have shown that positive values, which approach the experimental ones, are obtainable by using a realistic nuclear model. In both these papers shell-model wave functions are used with the harmonic oscillator parameters

fitted to give the proper r.m.s. radius [37] or from $p-2p$ and $e-ep$ experiments [38]. The use of the more suitable nuclear model combined with the inclusion of relativistic terms leads to the positive values given in Figs. 27–30, and it should also be mentioned that the results are not sensitive to reasonable changes in the parameters of the nuclear model. On the other hand, increasing the weak pseudoscalar coupling (whose value is not very well established) by 20%, increases [38] the asymmetry by some 30%. In these papers the final state interaction is taken into account as described in Section 2.3, but the authors concluded that it has little effect on the neutron asymmetry. A similar conclusion is reached [38] concerning the spin-orbit interaction, although on this point there is no confirmation from the work of Bouyssy et al. [97], whose calculation is moderately sensitive to such a term. The model of Madurga [92] gives for α in Ca a monotonically increasing function of energy, changing between 0.09 and 0.23 for E_n between 10 and 50 MeV.

Bouyssy and Vinh Nau have also checked [82] the insensitivity of the asymmetry of neutrons emitted after polarized muon capture in O^{16} and Ca^{40} to various nuclear models, by considering a pure shell-model and multi-hole-multi-particle configuration-mixing nuclear wave functions. On the other hand, in contradiction to previous conclusions [37, 38], they find in their treatment of the final state interaction that the addition of a surface term to the imaginary part of the optical potential affects considerably the energy dependence of α. In fact, they find an energy dependence (Fig. 32, curve 6) which reproduces fairly well the magnitude and overall behaviour of $\alpha(E_n)$, as given by Edelstein and Sundelin [33] (Fig. 31). However, the neutron intensity spectrum obtained by using the parameters used in calculating curve 6 of Fig. 32 compares poorly with the experimental findings. The agreement is markedly improved when they use [91] for Ca the wave functions of Campi and Spring [94], which are Hartree-Fock wave functions for a density dependent effective nucleon-nucleon interaction, while at the same time the asymmetry parameter does not change significantly from that given by curve 6 of Fig. 32.

Eramzhyan and Salganic [99] confirm large effects of the final state interaction on the neutron asymmetry in a calculation of $\mu + {}^{16}O \rightarrow {}^{15}N + n + \nu$. They consider the transitions to the ground state of ^{15}N and to three of its excited levels. Using the distorted wave approximation for the final state, they find marked differences compared to a plane wave approximation, the asymmetry becoming an oscillating function of E_n. This feature is quite stable against slight changes in the parameters of the optical potential. Thus, the question

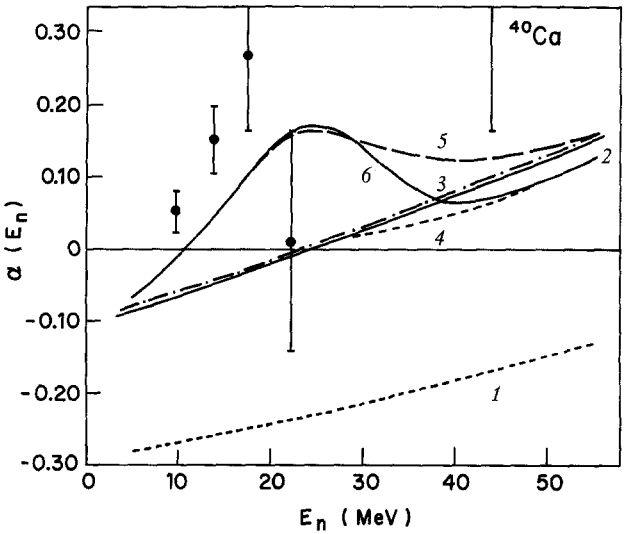

Fig. 32. Calculated (Ref. [82]) neutron asymmetry coefficient for Ca^{40}. Curve *1*: shell-model without relativistic corrections and without f.s.i. Curve *2*: same model with first order relativistic terms and real optical potential. Curve *3*: same as curve *2* but in configuration mixing model. Curve *4*: same as curve *2* plus volume absorption. Curve *5*: same as curve *2* plus surface absorption. Curve *6*: same as curve 2 plus volume and surface absorption

of the sensitivity of α to the final state interaction is certainly an open one so far.

Turning now to the γ-asymmetry, we recall [77] that γ-rays from the radiative capture $\mu^- + p \rightarrow n + \nu_\mu + \gamma$ should be emitted because of parity violation with an asymmetric distribution

$$N(\theta) = 1 + P_\mu \alpha_\gamma \cos\theta_{\gamma\mu}\,, \tag{23}$$

where P_μ is the muon polarization, $\theta_{\gamma\mu}$ the angle between the γ-momentum and the μ spin polarization. The asymmetry parameter α_γ is equal to the γ-ray circular polarization, if only the muon radiation is taken into account and for V − A interaction one has $\alpha_\gamma = 1$. Nuclear effects reduce α_γ in radiative muon capture in nuclei, and Rood and Tolhoek [78] have calculated $\alpha_\gamma = 0.75$ for radiative muon capture in Ca^{40} averaged over the γ-energy interval between 57–75 MeV.

In a recent experiment [79] discussed at this conference by Dr. Rosenstein, Di Lella et al. report a measurement of the γ-asymmetry for γ-energies between 57–75 MeV as giving

$$\alpha_\gamma \leqq -0.32 \pm 0.48\,. \tag{24}$$

The equality holds for vanishing neutron asymmetry parameter $\alpha_n = 0$, the knowledge of which is required in order to separate the neutron

contamination. If Sundelin's [76] value for $\alpha(E_n \simeq 50\,\text{MeV})$ is used, then the value of α_γ could be as low as -0.6 ± 0.5. This is in gross disagreement with theoretical expectations. A recent calculation of Longuemare and Piketty [80] of the neutron asymmetry parameter for the most energetic neutrons emitted after μ-capture finds for its limiting value $\alpha = 0.70$, quite independent of the model used. Their result thus aggravates the puzzle raised by the experiment of DiLella, Hammerman and Rosenstein.

References

1. MacDonald, B., Diaz, J. A., Kaplan, S. N., Pyle, R. V.: Phys. Rev. **139**, B 1253 (1965). Earlier experimental work on the average neutron emission is referred to here in Table V.
2. Ball, W., Lauterjung, K. H.: Z. Naturforsch. **8** A, 214 (1953).
3. Sundelin, R. M., Edelstein, R. M., Suzuki, A., Takahashi, K.: Phys. Rev. Letters **20**, 1198 (1968).
4. Krieger, M. H.: Thesis, Columbia University, NEVIS-172 (1969).
5. Schröder, W. U.: Thesis, Technische Hochschule Darmstadt (1971); – Jahnke, U. *et al.*: CERN preprint; – Schröder, W. U., Jahnke, U., Lindenberger, K. H., Röschert, G.: Darmstadt preprint (May 1973).
6. Balashov, V. V., Belyaev, V. B., Kabachnik, N. M., Eramzhian, R. A.: Phys. Letters **9**, 168 (1964).
7. Foldy, L. L., Walecka, J. D.: Nuovo Cimento **34**, 1026 (1964).
8. Überall, H.: Suppl. Nuovo Cimento **4**, 781 (1966).
9. Evseev, V., Kozlovski, T., Roganov, V., Woitkowska, J.: In: Devons, S. (Ed.): High-energy physics and nuclear structure, p. 157. New York: Plenum Press 1970. – Wojtkowska, J., Evseev, V. S., Kozlovski, T., Mamedov, T. N., Roganov, V. S.: Yad. Fiz. **14**, 624 (1971) [Soviet. J. Nucl. Phys. **14**, 349 (1972)]. – Wojtkowska, J., Evseev, V. S., Kozlovski, T., Roganov, V. S.: Yad. Fiz. **15**, 1154 (1972) [Sov. J. Nucl. Phys. **15**, 639 (1972)].
10. Tiomno, J., Wheeler, J. A.: Rev. Mod. Phys. **21**, 153 (1949).
11. Kaplan, S. N., Moyer, B. J., Pyle, R. V.: Phys. Rev. **112**, 968 (1958).
12. Brueckner, K. A., Gammel, J. L.: Phys. Rev. **109**, 1023 (1958).
13. Singer, P.: Nuovo Cimento **23**, 669 (1962).
14. Brueckner, K. A., Lockett, A. M., Rotenberg, M.: Phys. Rev. **121**, 255 (1961).
15. Weisskopf, V. F., Ewing, D. H.: Phys. Rev. **57**, 472 (1940).
16. Singer, P.: Phys. Rev. **124**, 1602 (1961).
17. Turkevich, A., Fung, S. C.: Phys. Rev. **92**, 521 (1953). – Winsberg, L.: Phys. Rev. **95**, 205 (1954).
18. Backenstoss, G., Charalambus, S., Daniel, H., Hamilton, W. D., Lynen, U., v. d. Malsburg, Ch., Poelz, G., Povel, H. P.: Nucl. Phys. A **162**, 541 (1971).
19. Petitjean, C., Backe, H., Engfer, R., Jahnke, U., Lindenberger, K. H., Schneuwly, H., Schröder, W. U., Walter, H. K.: Nucl. Phys. A **178**, 193 (1971).
20. Kessler, D., McKee, R. J., Hargrove, C. K., Hincks, E. P., Anderson, H. L.: Canad. J. Phys. **48**, 3029 (1970).
21. Pratt, T. A. E. C.: Nuovo Cimento **61** B, 119 (1969).
22. Earle, E. D., Bartholomew, G. A.: Nucl. Phys. A **176**, 363 (1971).
23. Bunatyan, G. G., Evseev, V. S., Nikityuk, L. N., Nikolina, A. A., Pokrovskii, V. N., Roganov, V. S., Smirnova, L. M., Yutlandov, I. A.: Yad. Fiz. **9**, 783 (1969); [Soviet J. Nucl. Phys. **9**, 457 (1969)].

24. Bunatyan, G.G., Evseev, V.S., Nikityuk, L.N., Pokrovskii, V.N., Rybakov, V.N., Yutlandov, I.A.: Yad. Fiz. **11**, 795 (1970); [(Soviet J. Nucl. Phys. **11**, 444 (1970)].
25. Raphael, R., Überall, H., Werntz, C.: Phys. Letters **24B**, 15 (1967).
26. Kelly, F.J., Überall, H.: Nucl. Phys. A**118**, 302 (1968).
27. See also Pratt, T.A.E.C.: Nuovo Cimento **68**A, 477 (1970).
28. Evseev, V., Kozlowski, T., Roganov, V., Wojtkowska, J.: Phys. Letters **28**B, 553 (1969).
29. Plett, M.E., Sobottka, S.E.: Phys. Rev. C **3**, 1003 (1971).
30. Singer, P., Zin, A.: to be published.
31. Hagge, D.: Thesis. University of California, UCRL–10516 (1963).
32. Turner, L.: Thesis. Carnegie Institute of Technology, CAR-882-5 (1964).
33. Sundelin, R.M.: Thesis. Carnegie Institute of Technology, CAR-882-22 (1967). – Sundelin, R.M., Edelstein, R.M.: Phys. Rev. C **7**, 1037 (1973).
34. Überall, H.: Nuovo Cimento **6**, 533 (1957).
35. Lubkin, E.: Ann. Phys. **11**, 414 (1960).
36. Dolinsky, E.I., Blokhintsev, L.D.: Nucl. Phys. **10**, 527 (1959).
37. Bogan, A.: Phys. Rev. Letters **22**, 71 (1969). – Nucl. Phys. B**12**, 89 (1969).
38. Piketty, C.A., Procureur, J.: Nucl. Phys. B **26**, 390 (1971).
39. Klein, R., Neal, T., Wolfenstein, L.: Phys. Rev. **138**, B 86 (1965).
40. Akimova, M.K., Blokhintsev, L.D., Dolinskii, E.I.: J. Exptl. Theoret. Phys. (U.S.S.R.) **39**, 1806 (1960); [Sov. Phys. JETP **12**, 1260 (1961)].
41. Novikov, V.M., Urin, M.G.: Yad. Fiz. **6**, 1233 (1967); [Soviet J. Nucl. Phys. **6**, 898 (1968)].
42. Fujii, A., Primakoff, H.: Nuovo Cimento **12**, 327 (1959).
43. Moniz, E.J.: Phys. Rev. **184**, 1154 (1969). – Moniz, E.J., Sick, I., Whitney, R.R., Ficenec, J.R., Kephart, R.D., Trower, W.P.: Phys. Rev. Letters **26**, 445 (1971).
44. Gilbert, A., Cameron, A.G.W.: Canad. J. Phys. **43**, 1446 (1965).
45. Morinaga, H., Fry, W.F.: Nuovo Cimento **10**, 308 (1953).
46. Kotelchuck, D.: Nuovo Cimento **35**, 27 (1964).
47. Vaisenberg, A.O., Kolganova, E.D., Rabin, N.V.: Yad. Fiz. **1**, 652 (1965) [Soviet J. Nucl. Phys. **1**, 467 (1965)].
48. Vaisenberg, A.O., Kolganova, E.D., Rabin, N.V.: Yad. Fiz. **11**, 830 (1970) [Soviet J. Nucl. Phys. **11**, 464 (1970)].
49. Ishii, C.: Prog. Theor. Phys. **21**, 663 (1959).
50. Kotelchuk, D., McEwen, J.G., Orear, J.: Phys. Rev. **129**, 876 (1963).
51. Kotelchuk, D., Tyler, J.V.: Phys. Rev. **165**, 1190 (1968).
52. Endt, P.M., Demeur, M., (Ed.): Nuclear reactions, Vol. I, Chaps. VII, IX. Amsterdam: North Holland Publ. Co. 1959.
53. Kawai, M., Kikuchi, K.: Nuclear matter and nuclear reactions. Amsterdam: North Holland Publ. Co. 1968.
54. Bertero, M., Passatore, G., Viano, G.A.: Nuovo Cimento **38**, 1669 (1965).
55. Wilkinson, D.H., In: Birks, J.B., (Ed.): Proc. of the Rutherford Jubilee Inter. Conf., p. 339 London: Heywood & Co. 1961.
56. Tagami, T.: Prog. Theor. Phys. **21**, 465 (1959).
57. da Providencia, J.: Proc. Phys. Soc. **77**, 81 (1961).
58. Überall, H., Wolfenstein, L.: Nuovo Cimento **10**, 136 (1958).
59. Hodgson, P.E.: Nucl. Phys. **8**, 1 (1958).
60. Elton, L.R.B., Gomes, L.C.: Phys. Rev. **105**, 1027 (1957).
61. Oda, N., Harada, K.: Nucl. Phys. **7**, 251 (1958).
62. Feshbach, H., Shapiro, M.M., Weisskopf, V.F.: USAEC Report NY03077 (1953).
63. Bertero, M., Passatore, G., Viano, G.A.: Nuovo Cimento **52**, 1379 (1967).
64. Siegert, A.J.F.: Phys. Rev. **52**, 787 (1937).
65. Sachs, R.G., Austern, N.: Phys. Rev. **81**, 705 (1951).
66. See, e.g. Schopper, H.F.: Weak interactions and nuclear beta decay. Amsterdam: North Holland Publ. Co., 1966.

67. Sobottka, S.E., Wills, E.L.: Phys. Rev. Letters **20**, 596 (1968).
68. Vil'gel'mova, L., Evseev, V.S., Nikityuk, L.N., Pokovskii, V.N., Yutlandov, I.A.: Yad. Fiz. **13**, 551 (1971); [Soviet J. Nucl. Phys. **13**, 310 (1971)].
69. See also Charalambus, S.: Nucl. Phys. A**166**, 145 (1971).
70. Budyashov, Yu.G., Zinov, V.G., Konin, A.D., Mukhin, A.I., Chatrchyan, A.M.: Zh. Eksp. Teor. Fiz. **60**, 19 (1971) [Soviet Physics JETP **33**, 11 (1971)].
71. Dostrovsky, I., Fraenkel, Z., Weinberg, L.: Phys. Rev. **118**, 781 (1960).
72. See, e.g. Rho, M.: Lectures at Les Houches Summer School of Theoretical Physics (1968).
73. Primakoff, H.: Rev. Mod. Phys. **31**, 802 (1959).
74. Evseev, V., Roganov, V., Chernogorova, V., Chang Jun-wa, Szymczak, M.: Phys. Letters **6**, 332 (1963). – Evseev, V., Kilbinger, F., Roganov, V., Chernogorova, V., Szymczak, H.: Yad. Fiz. **4**, 545 (1967) [Soviet J. Nucl. Phys. **4**, 387 (1967)].
75. Sculli, J.: Thesis. Columbia University (1969).
76. Sundelin, R.M., Edelstein, R.M., Suzuki, A., Takahashi, K.: Phys. Rev. Letters **20**, 1201 (1968).
77. A detailed account on radiative muon capture can be found in Rood, H.P.C.: Thesis. Rijksuniversiteit te Groningen (1964).
78. Rood, H.P.C., Tolhoek, H.A.: Nucl. Phys. **70**, 658 (1965); see also Borchi, E., De Gennaro, S.: Phys. Rev. C**2**, 1012 (1970), who obtain slightly larger values for α_{γ}.
79. DiLella, L., Hammerman, I., Rosenstein, L.M.: Phys. Rev. Letters **27**, 830 (1971).
80. Longuemare, C., Piketty, C.A.: Phys. Letters **38**B, 125 (1972).
81. Überall, H.: Springer Tracts in Mod. Phys. (to be published).
82. Bouyssy, A., Vinh Mau, N.: Nucl. Phys. A**185**, 32 (1972).
83. Bobodyanov, I.: Acta Phys. Acad. Sci. Hung. **29**, Supple. 4, 151 (1970).
84. Evans, H.J.: Nucl. Phys. A**207**, 379 (1973).
85. Temple, L.E., Kaplan, S.N., Pyle, R.V., Valley, G.F.: LBL 24 (1971). – Temple, L.E.: Thesis, LBL 781 (1972).
86. Miller, G.H., Eckhause, M., Martin, P., Welsh, R.E.: Phys. Rev. C**6**, 487 (1972).
87. Lucas, G.R., Jr., Martin, P., Miller, G.H., Welsh, R.E., Jenkins, D.A., Powers, R.J., Kunselman, A.R.: Phys. Rev. C**7**, 1678 (1973).
88. Bunatyan, G.G., Vie'gel'mova, L., Evseev, V.S., Nikityuk, L.N., Pokrovskii, V.W., Rybakov, V.N., Yutlandov, I.A.: Yad. Fiz. **15**, 945 (1972) [Soviet J. Nucl. Phys. **15**, 526 (1972)].
89. Kaplan, S.N.: In: Devons, S., (Ed.): High energy physics and nuclear structure, p. 143. New York: Plenum Press.
90. Heusser, G., Kirsten, T.: Nucl. Phys. A**195**, 369 (1972).
91. Bouyssy, A., Ngo, H., Vinh Mau, N.: Phys. Letters **44**B, 139 (1973).
92. Madurga, G.: Nuovo Cimento **12**A, 451 (1972).
93. Komarov, V.I., Savchenko, O.V.: Yad. Fiz. **8**, 415 (1968) [Soviet J. Nucl. Phys. **8**, 239 (1969)].
94. Wojtkowska, I., Evseev, V.S., Kozlowski, T., Nikolina, A.A., Roganov, V.S.: Yad. Fiz. **15**, 939 (1972) [Soviet J. Nucl. Phys. **15**, 523 (1972)].
95. Madurga, G.: Nuovo Cimento **12**A, 451 (1972).
96. Galindo, A., Pascual, P., Pascual, R.: Anal. Fisica (Spain) **68**, 275 (1972).
97. Bouyssy, A., Ngo, H., Vinh Mau, N.: Phys. Letters **44**B, 139 (1973).
98. Campi, X., Sprung, D.W.L.: Nucl. Phys. A**194**, 401 (1972).
99. Eramzhyan, R.A., Salganic, Yu.A.: Nucl. Phys. A**207**, 609 (1973).

Prof. Dr. Paul Singer
Department of Physics
Technion – Israel Institute of Technology
Haifa, Israel